SUPPORTING INFORMATION

In silico assisted identification, synthesis and *in vitro* pharmacological characterization of potent and selective blockers of the epilepsy-associated KCNT1 channel

Nunzio Iraci, [‡,#] Lidia Carotenuto,[¶,#] Tania Ciaglia,[₸,#] Giorgio Belperio,[¥,#] Francesca Di Matteo, [₸] Ilaria Mosca,[ǁ] Giusy Carleo,[¶] Manuela Basilicata,[^] Paolo Ambrosino,[¥] Rita Turcio, [₸] Deborah Puzo,[ǁ] Giacomo Pepe,[₸] Isabel Gomez-Monterrey,[§] Maria Virginia Soldovieri,[ǁ] Veronica Di Sarno,[₸] Pietro Campiglia,[₸] Francesco Miceli,[¶] Alessia Bertamino,[₸] Carmine Ostacolo,[₸,*] Maurizio Taglialatela.[¶,*]

[‡] Department of Chemical, Biological, Pharmaceutical and Environmental Sciences (CHIBIOFARAM), University of Messina, Viale F. Stagno d'Alcontres 31, 98166, Messina, Italy
[¶] Department of Neuroscience, Reproductive Sciences and Dentistry, University Federico II of Naples, Via S. Pansini, 5, 80131, Naples, Italy
[₸] Department of Pharmacy, University of Salerno, Via G. Paolo II 132, 84084, Fisciano, SA, Italy
[^] Department of advanced Medical and Surgical Sciences, University of Campania "Luigi Vanvitelli", P.zza L. Miraglia 2, 80138, Naples, Italy
[¥] Department of Science and Technology, University of Sannio, Via F. De Sanctis, 82100, Benevento, Italy
[ǁ] Department of Medicine and Health Science, University of Molise, Via C. Gazzani, 86100, Campobasso, Italy
[§] Department of Pharmacy, University Federico II of Naples, Via D. Montesano 49, 80131, Naples, Italy

*Corresponding authors (Maurizio Taglialatela : maurizio.taglialatela@unina.it; Carmine Ostacolo : costacolo@unisa.it)
#Equal contribution

Table of content:

Compound	Chemical structure	Docking score (kcal/mol)	MW	SASA[a, c]	PSA[a, d]	HBDs[a, e]	HBAs[a, e]	LogP[a, f]	Chiral centers	Rotatable bonds [a, b]
CPK1 *[50]*	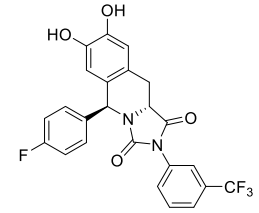	-11.200	472.395	692.726	101.373	2	5	4.738	2	2
CPK2	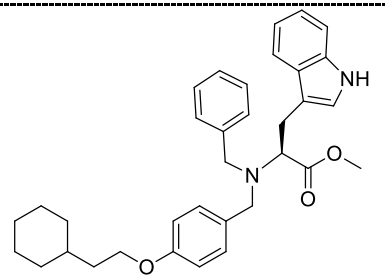	-12.444	524.702	956.515	53.335	1	4.75	7.966	1	12
CPK3	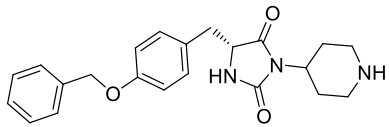	-11.033	379.458	680.787	86.184	2	5.75	3.517	1	5
CPK4 *[51]*	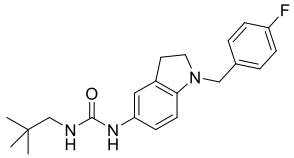	-10.328	355.454	683.486	49.646	2	3	4.261	0	5

Compound	Chemical structure	Docking score (kcal/mol)	MW	SASA[a, b]	PSA[a, c]	HBDs[a, d]	HBAs[a, d]	LogP[a, e]	Chiral centers	Rotatable bonds [a, f]
CPK5	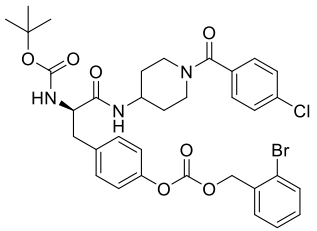	-11.173	715.039	1067.831	142.171	1.25	9.75	6.901	1	10
CPK6 *52*	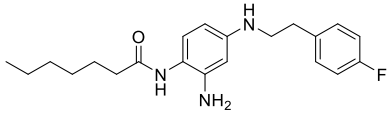	-11.388	357.47	740.999	73.336	3.5	4.5	4.586	0	11
CPK7	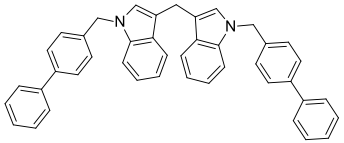	-13.156	578.755	1011.543	3.400	0	0	12.737	0	8
CPK8	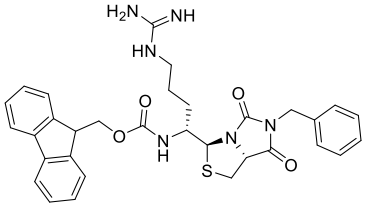	-12.576	598.718	960.68	167.577	5	8.5	5.442	3	11

Compound	Chemical structure	Docking score (kcal/mol)	MW	SASA[a, b]	PSA[a, c]	HBDs[a, d]	HBAs[a, d]	L[a, e]	Chiral centers	Rotatable bonds [a, f]
CPK9 *53*	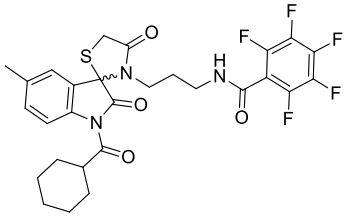	-10.434	595.583	845.541	111.409	1	9	4.985	1	6
CPK10	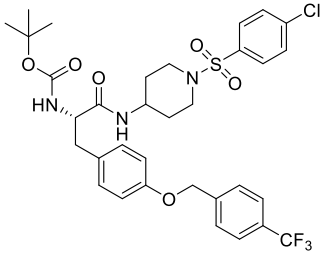	-12.710	696.18	1020.559	110.388	1.25	9.5	7.354	1	11
CPK11 *54*	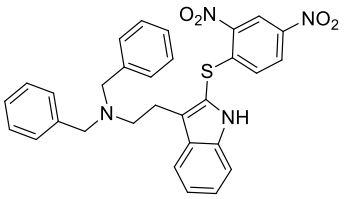	-10.744	538.62	887.828	107.651	1	4	6.684	0	11
CPK12 *55*	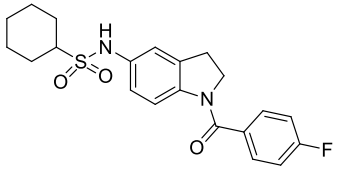	-10.828	402.483	682.372	76.427	1	7.5	3.374	0	4

Compound	Chemical structure	Docking score (kcal/mol)	MW	SASA[a, b]	PSA[a, c]	HBDs[a, d]	HBAs[a, d]	LogP[a, e]	Chiral centers	Rotatable bonds [a, f]
CPK13 *55*	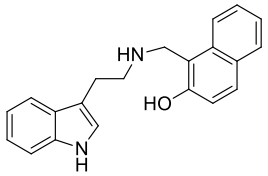	-10.154	316.402	607.332	44.605	3	2.25	4.109	0	6
CPK14 *56*	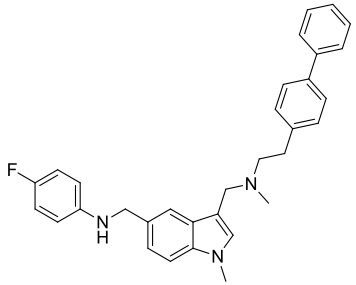	-12.02	477.623	830.959	17.447	1	3	8.157	1	9
CPK15 *57*	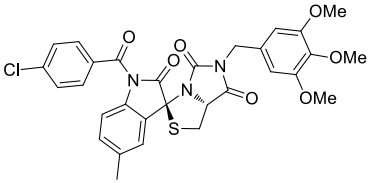	-10.178	608.064	887.55	128.404	0	9.25	5.548	2	6
CPK16 *57*	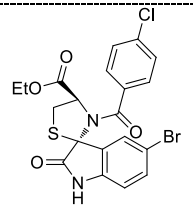	-10.139	495.774	649.802	91.815	1	8	3.712	2	3

Compound	Chemical structure	Docking score (kcal/mol)	MW	SASA[a, b]	PSA[a, c]	HBDs[a, d]	HBAs[a, d]	LogP[a, e]	Chiral centers	Rotatable bonds [a, f]
CPK17 [53]	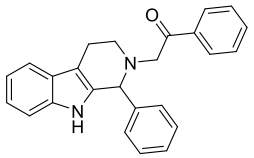	-11.027	366.462	670.154	40.916	1	4	4.971	1	3
CPK18	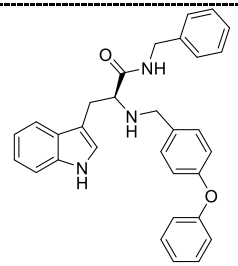	-13.347	475.589	809.766	63.395	3	4.5	5.778	1	10
CPK19	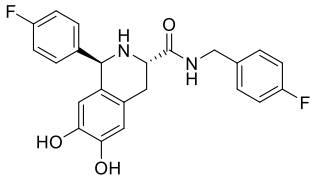	-11.721	410.419	706.564	92.584	4	5.5	2.816	2	5
CPK20 [51]	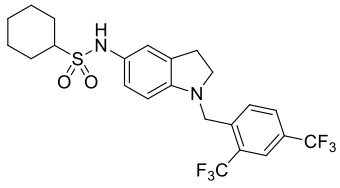	-10.733	506.505	736.689	47.879	1	5.5	5.409	0	5

Table S1: Characterizing chemical-physical parameters of the tested molecules**.** [a] Calculated by mean of QikProp [**Schrödinger Release 2019-1**: QikProp, Schrödinger, LLC, New York, NY, 2019.]; [b] Total solvent accessible surface area in square angstroms (probe radius 1.4 Å); [c] Polar surface area in square angstroms (probe radius 1.4 Å); [d] Hydrogen bond donors (HBDs) and acceptors (HBAs) counts are averaged over different states, so they can be non-integer; [e] QikProp-predicted octanol/water partition coefficient; [f] Trivial and hindered rotatable bonds are excluded from the count; The number in superscript represent the references to the synthesis of the corresponding derivatives reported in the main text.

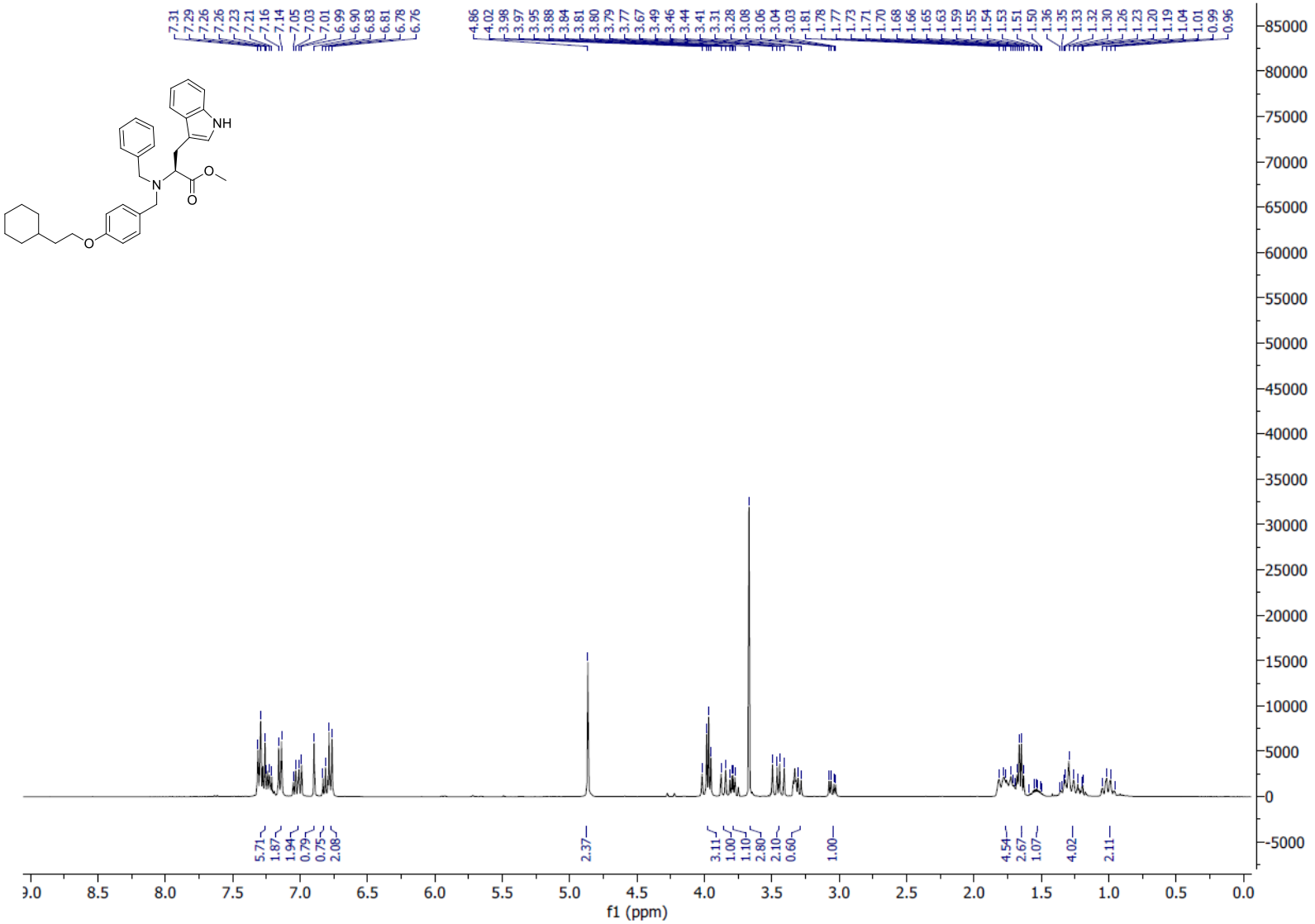

Figure S1: ^{1}H NMR spectra for compound **CPK2**

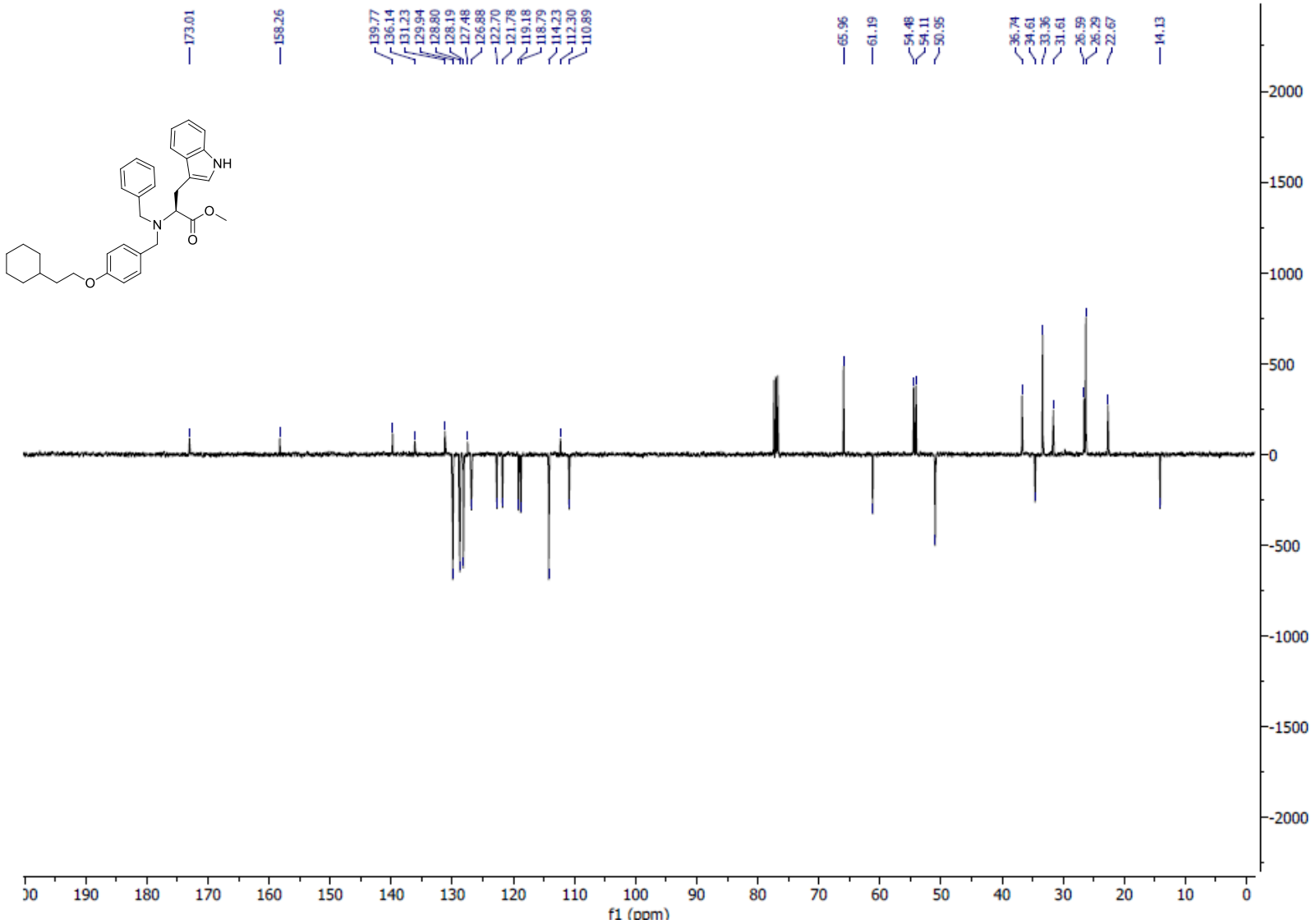

Figure S2: qDEPT NMR spectra for compound **CPK2**

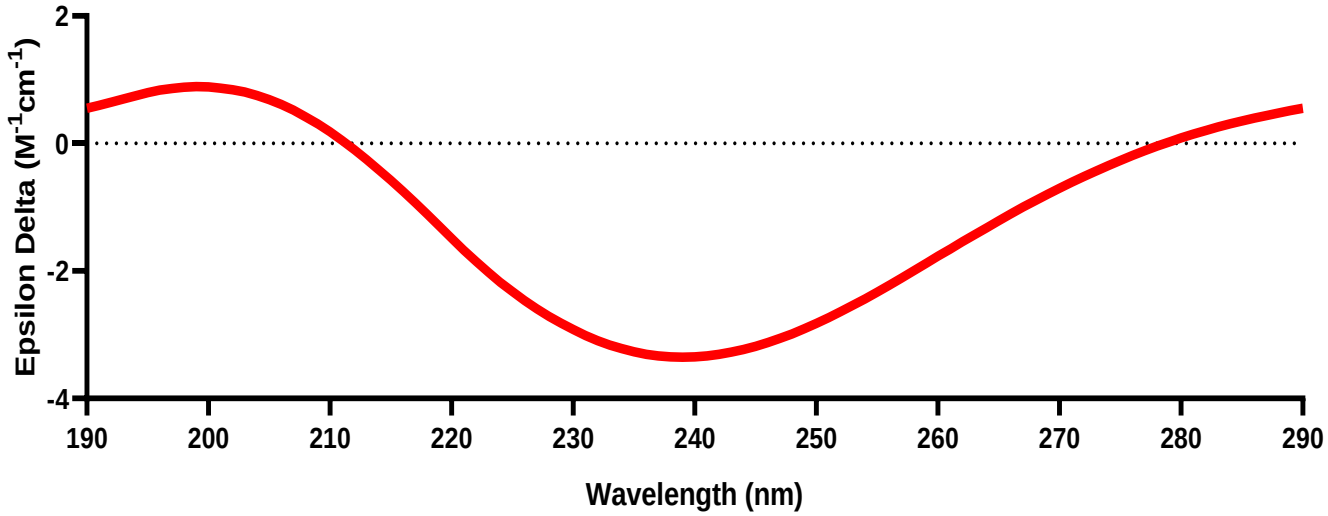

Figure S3: CD spectra for compound **CPK2**

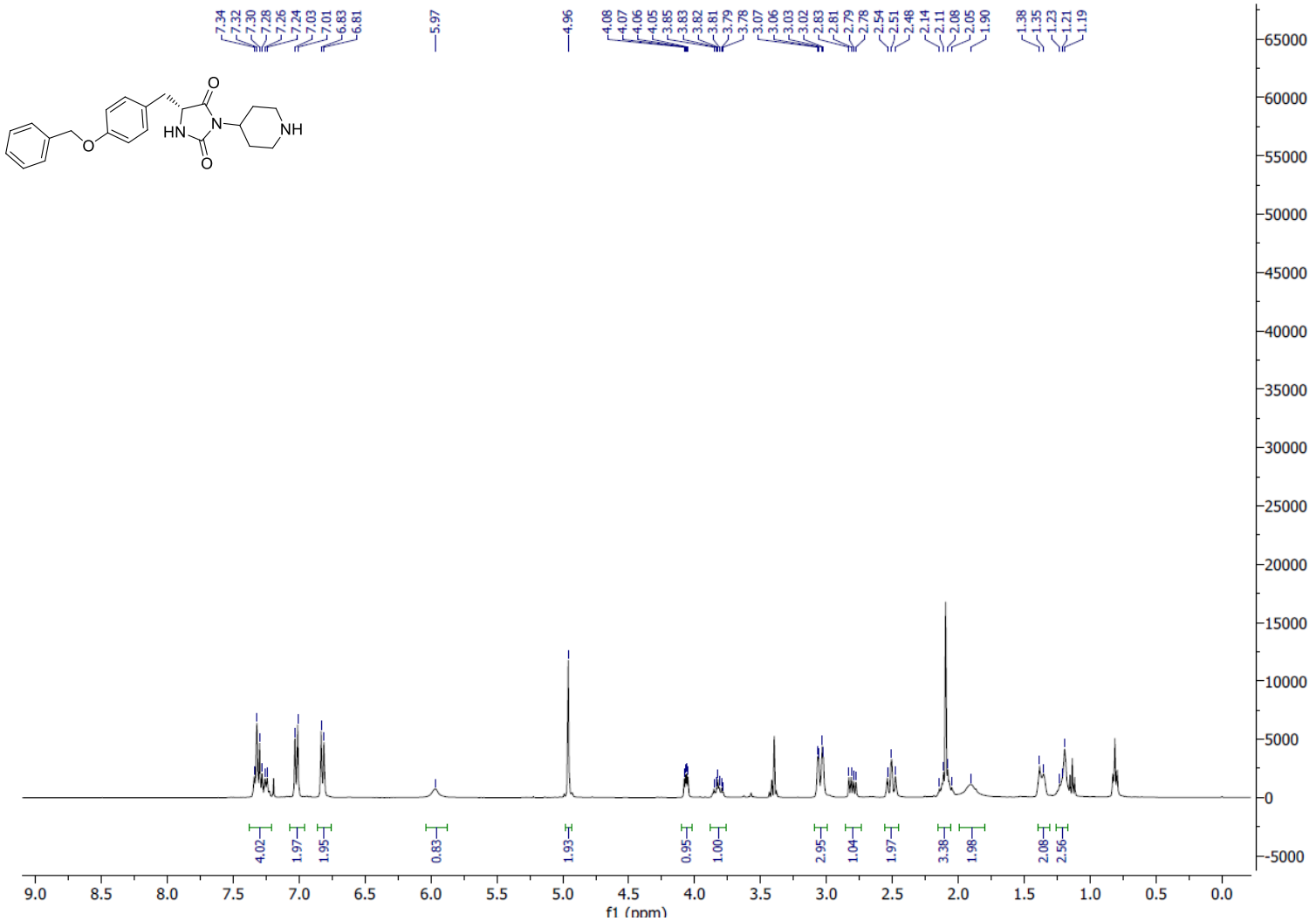

Figure S4: ^{1}H NMR spectra for compound **CPK3**

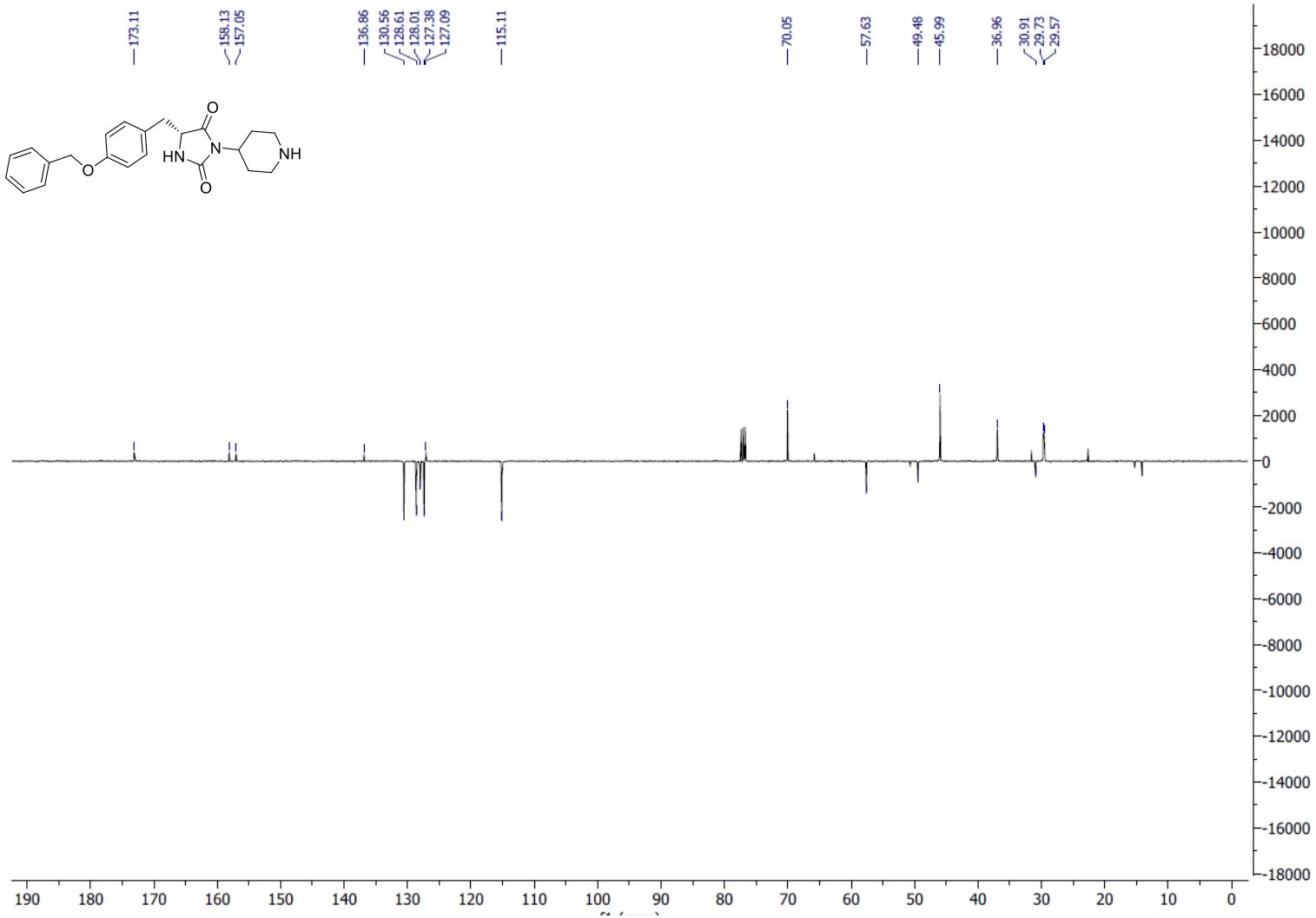

Figure S5: qDEPT NMR spectra for compound **CPK3**

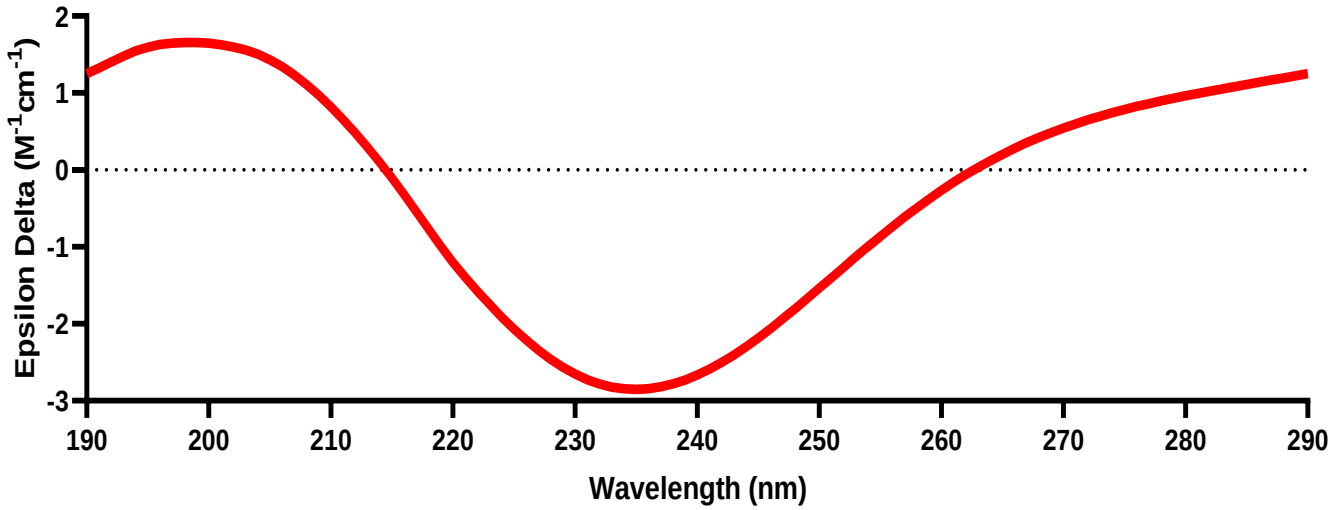

Figure S6: CD spectra for compound **CPK3**

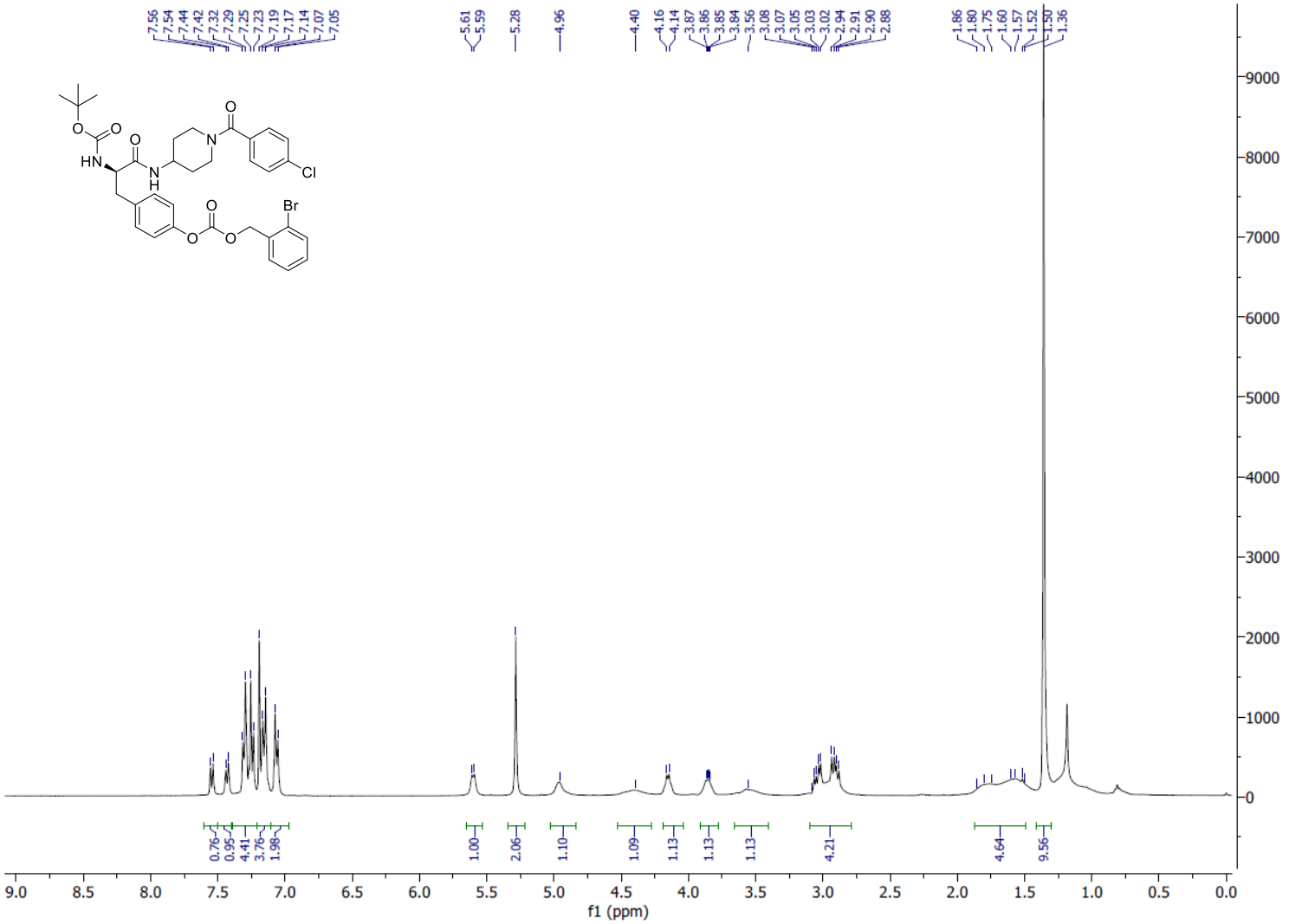

Figure S7: ^{1}H NMR spectra for compound **CPK5**

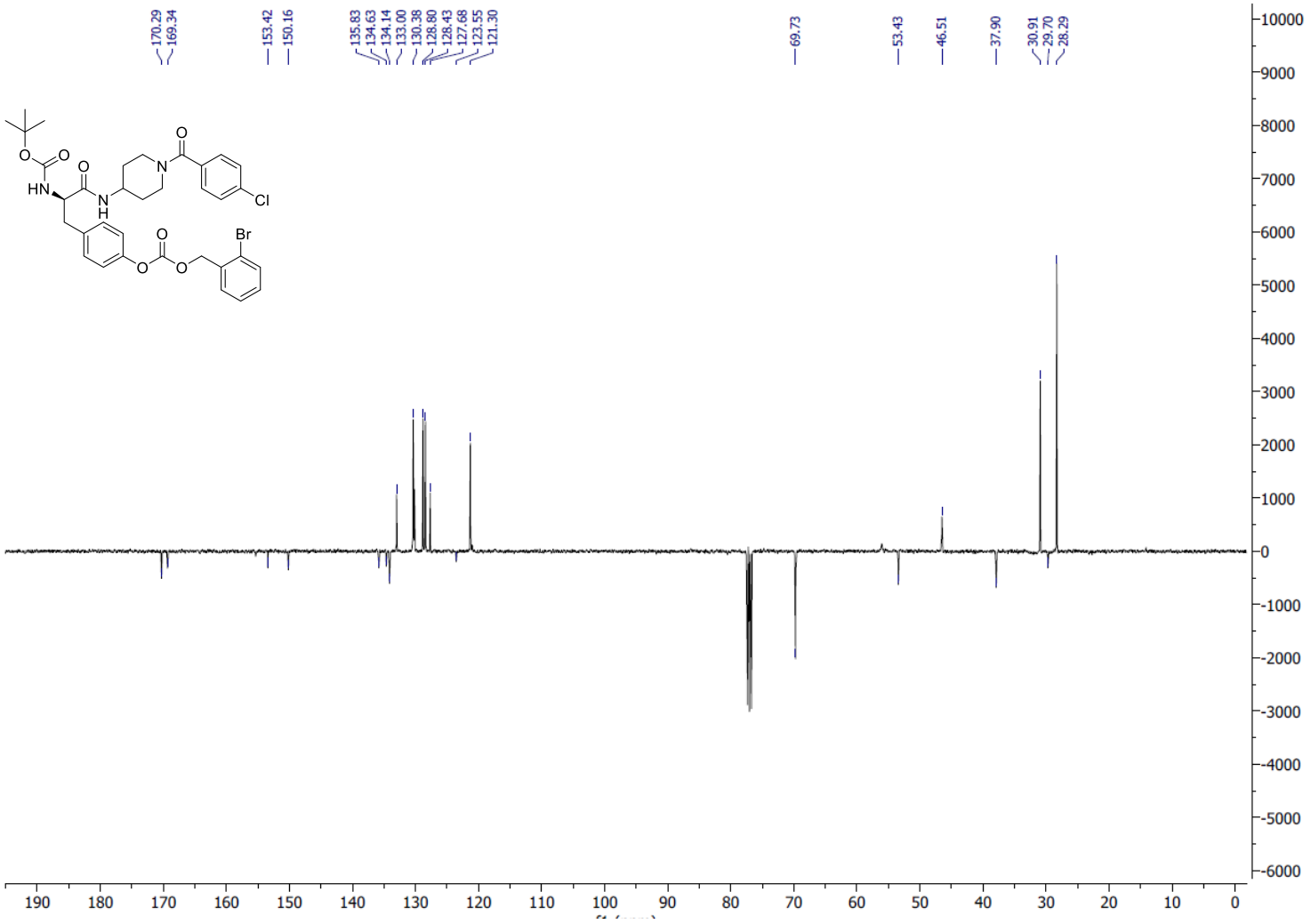

Figure S8: qDEPT NMR spectra for compound **CPK5**

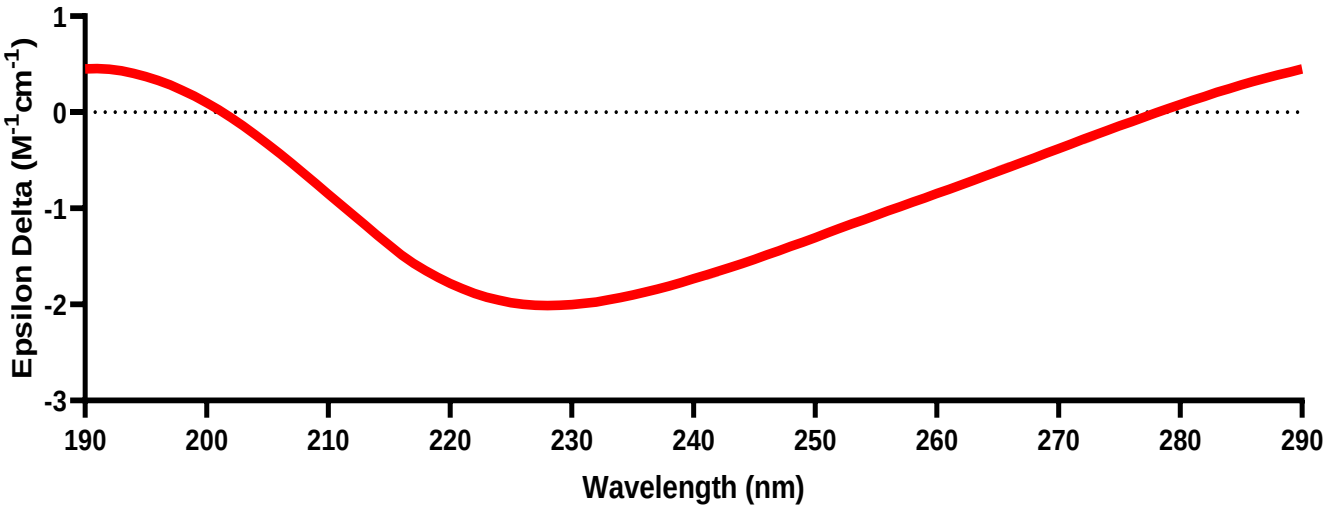

Figure S9: CD spectra for compound **CPK5**

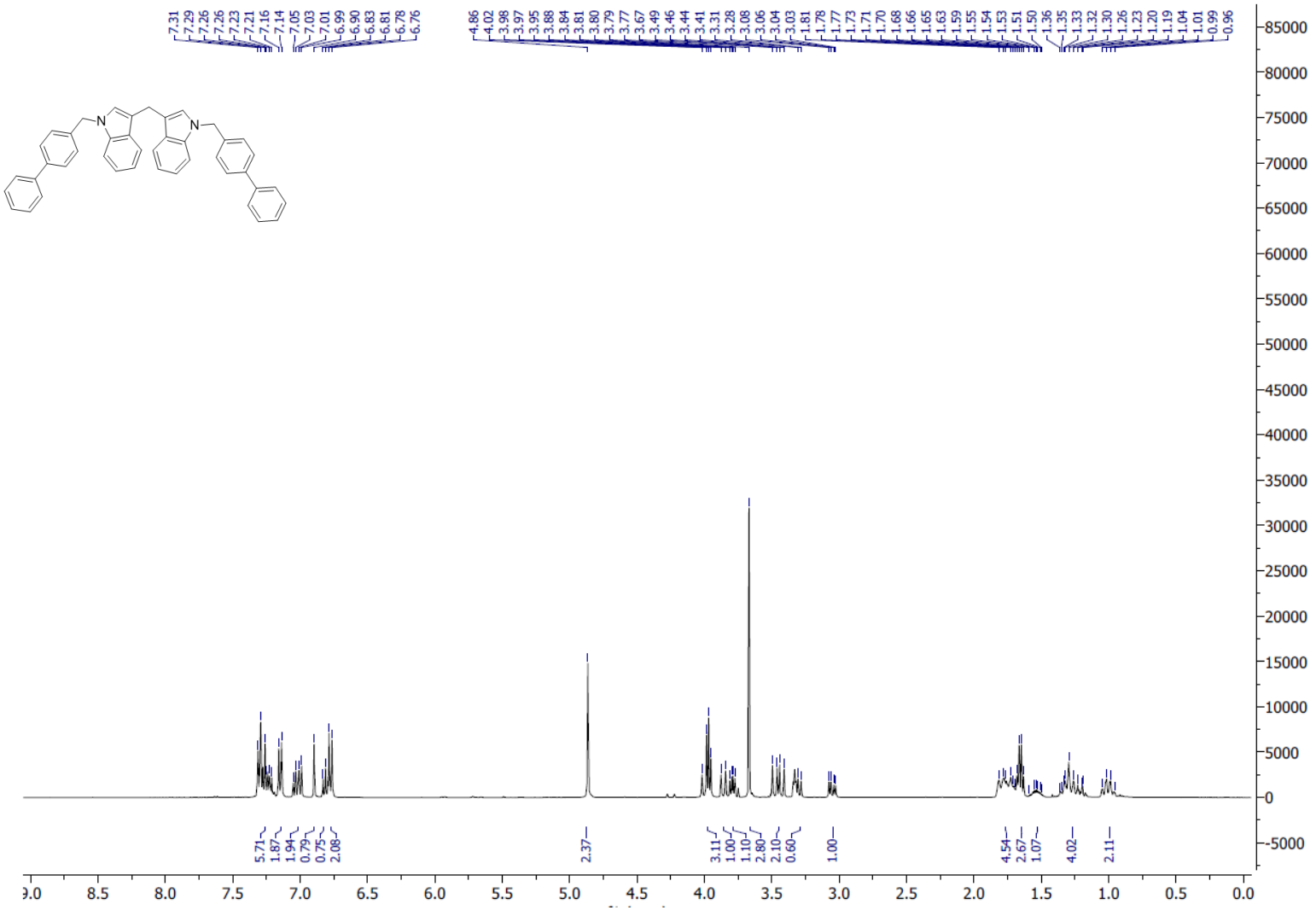

Figure S10: ^{1}H NMR spectra for compound **CPK7**

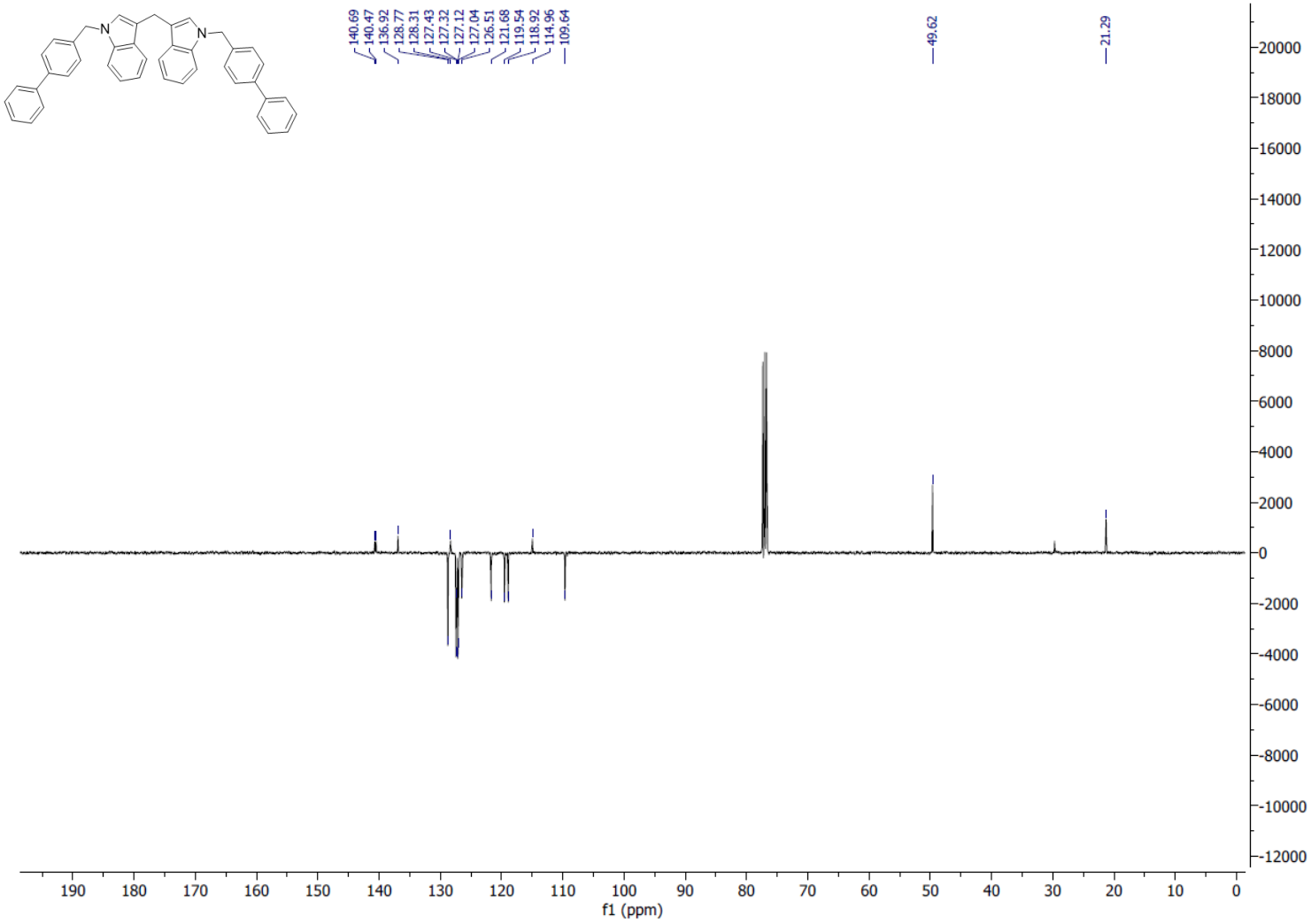

Figure S11: qDEPT NMR spectra for compound **CPK7**

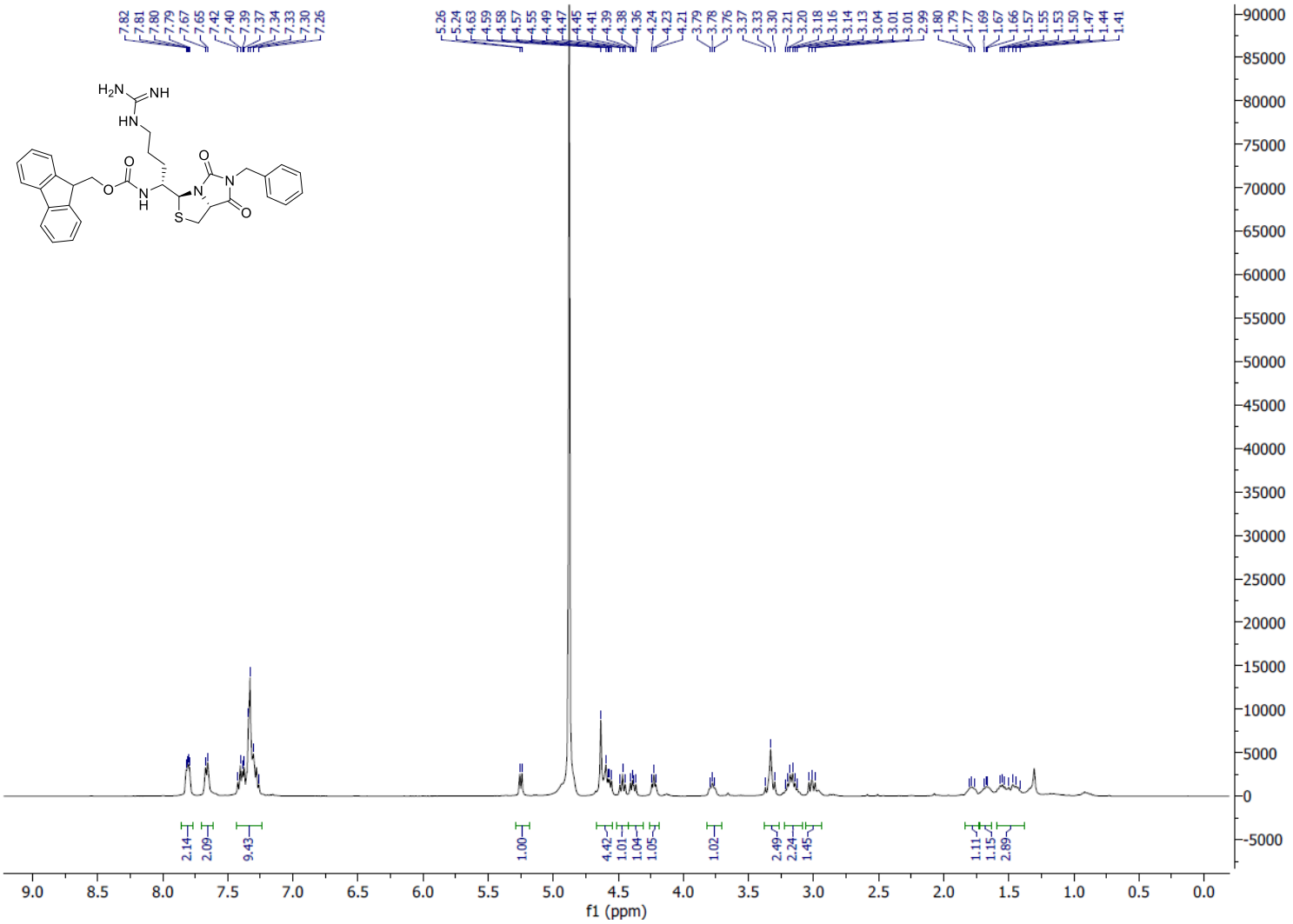

Figure S12: ^{1}H NMR spectra for compound **CPK8**

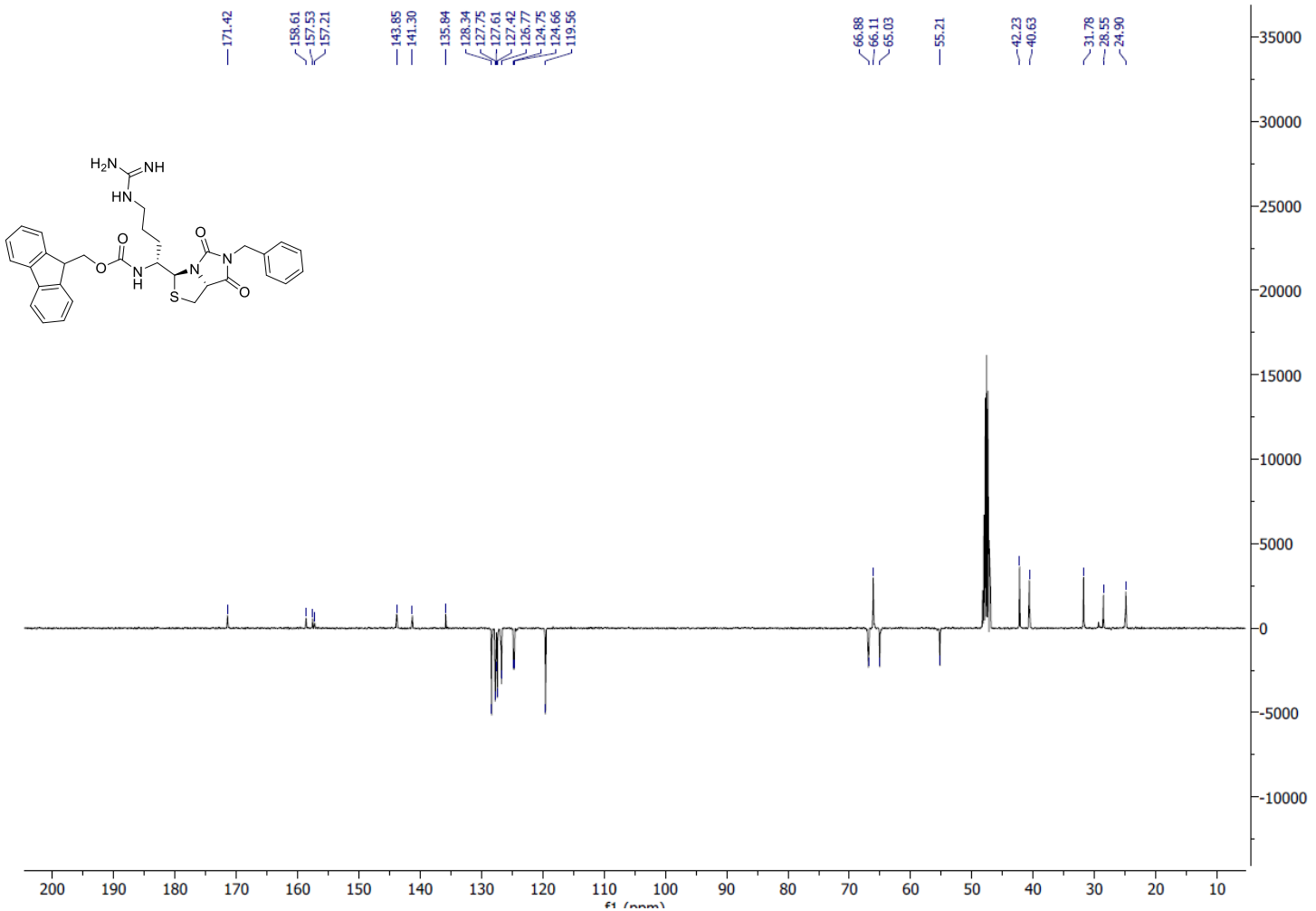

Figure S13: qDEPT NMR spectra for compound **CPK8**

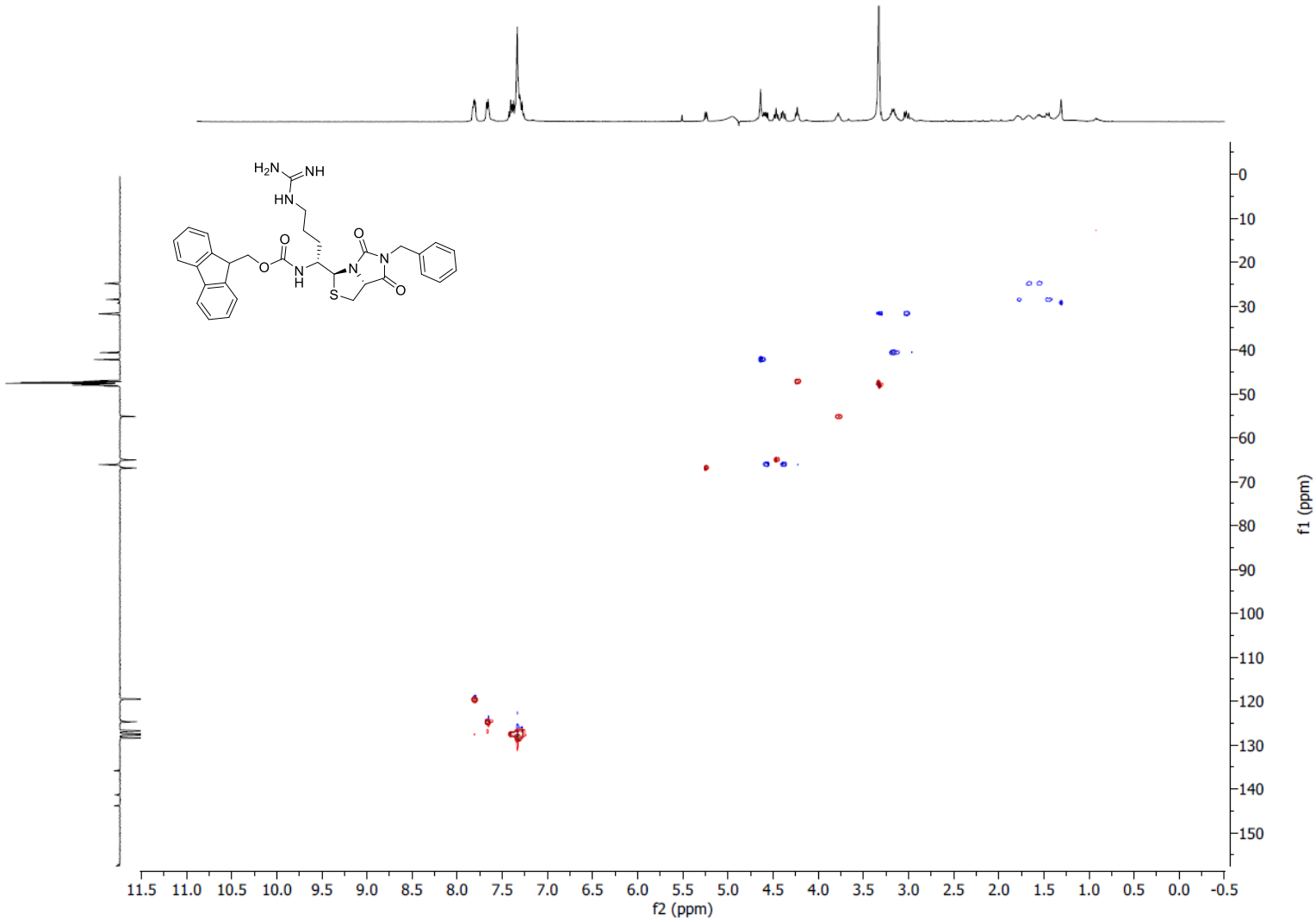

Figure S14: HSQC NMR spectra for compound **CPK8**

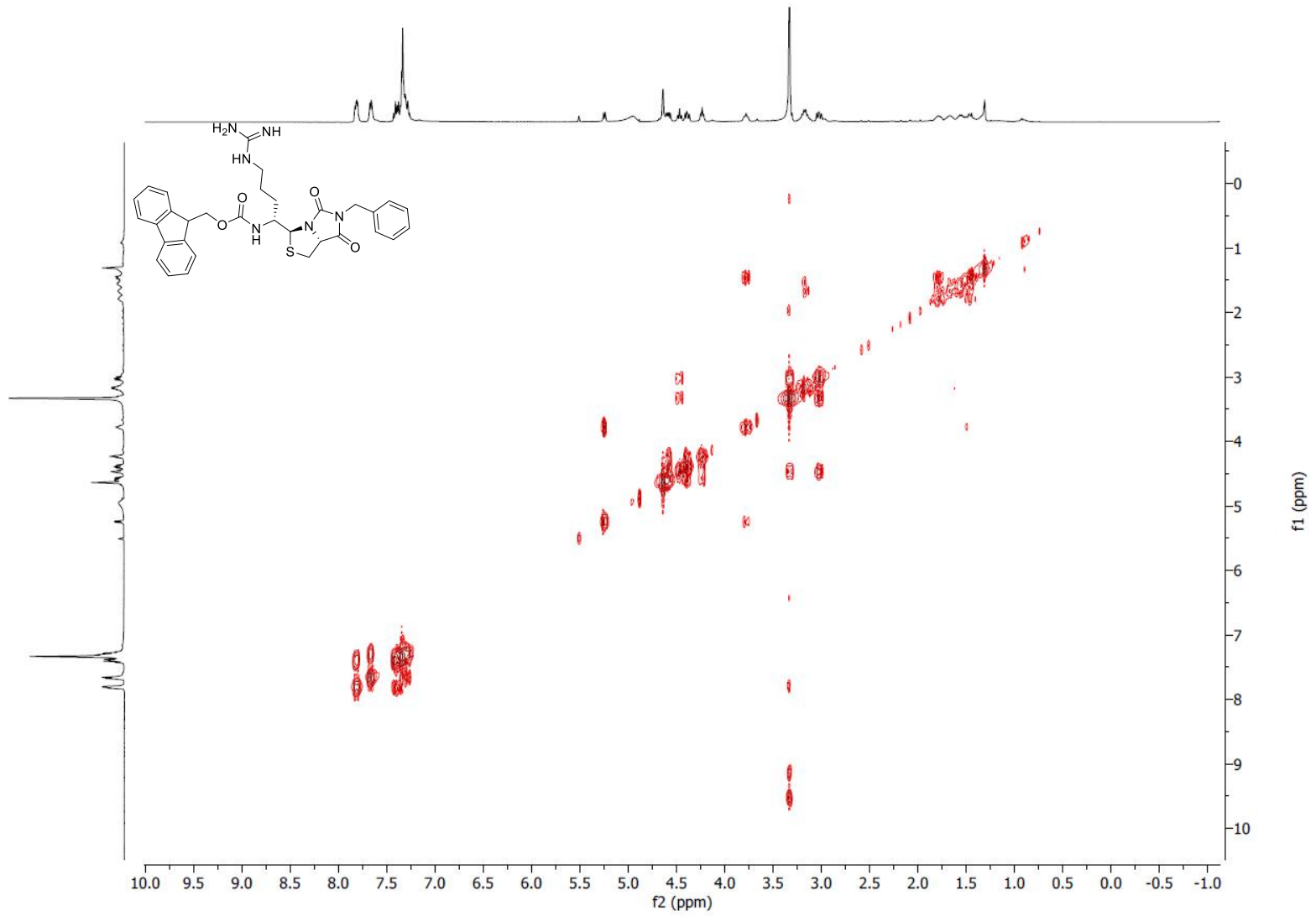

Figure S15: COSY NMR spectra for compound **CPK8**

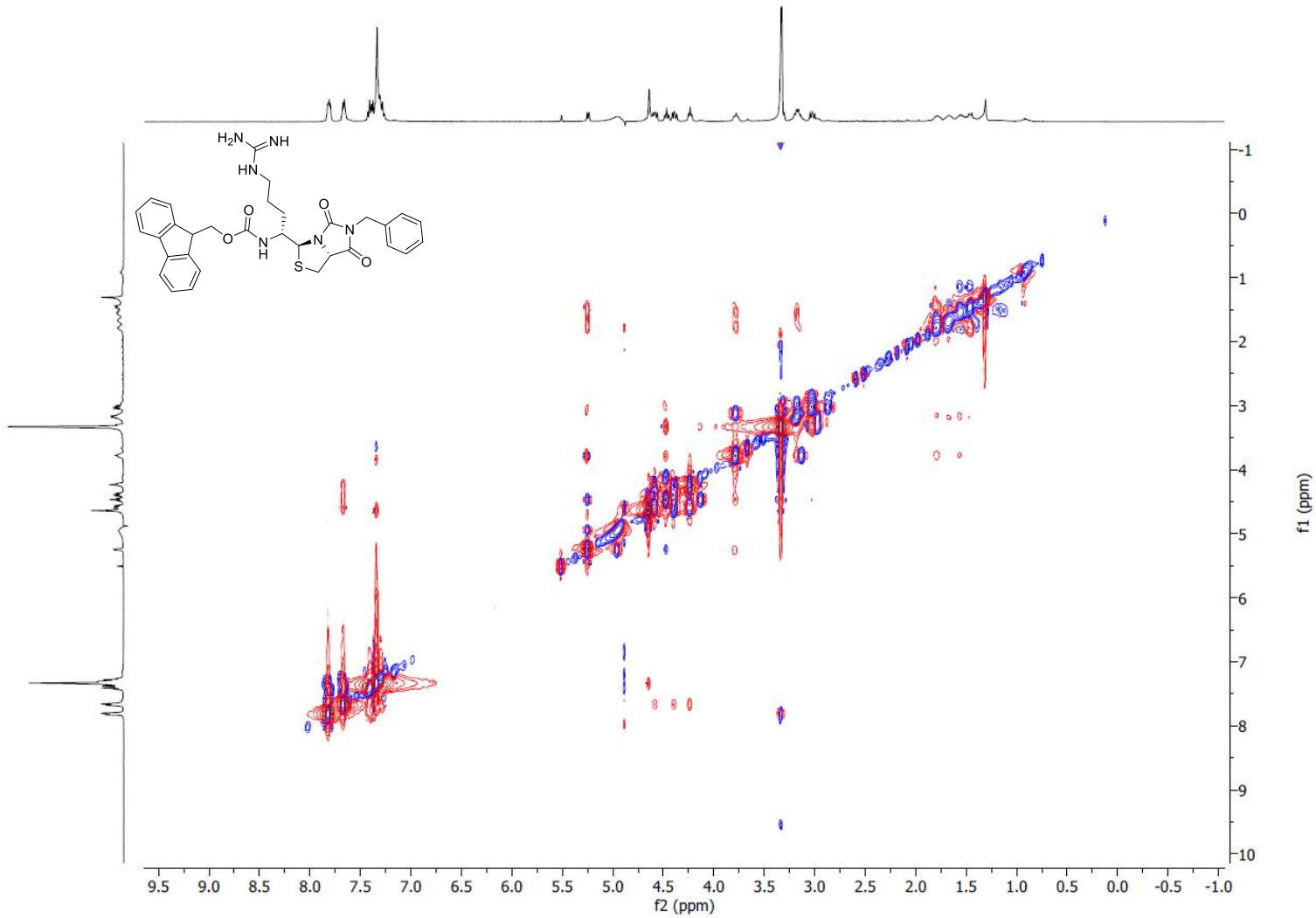

Figure S16: ROESY NMR spectra for compound **CPK8**

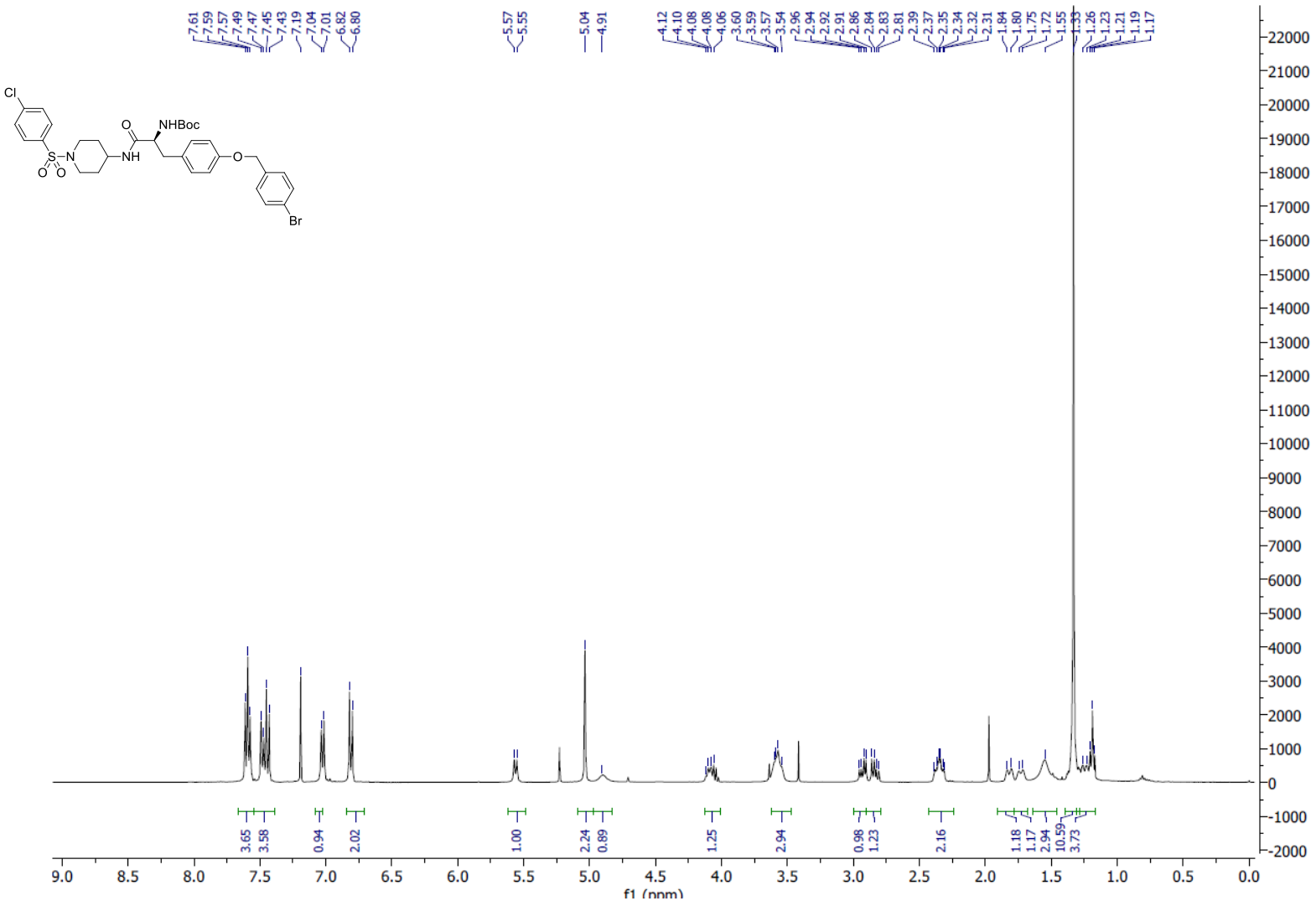

Figure S17: [1]H NMR spectra for compound **CPK10**

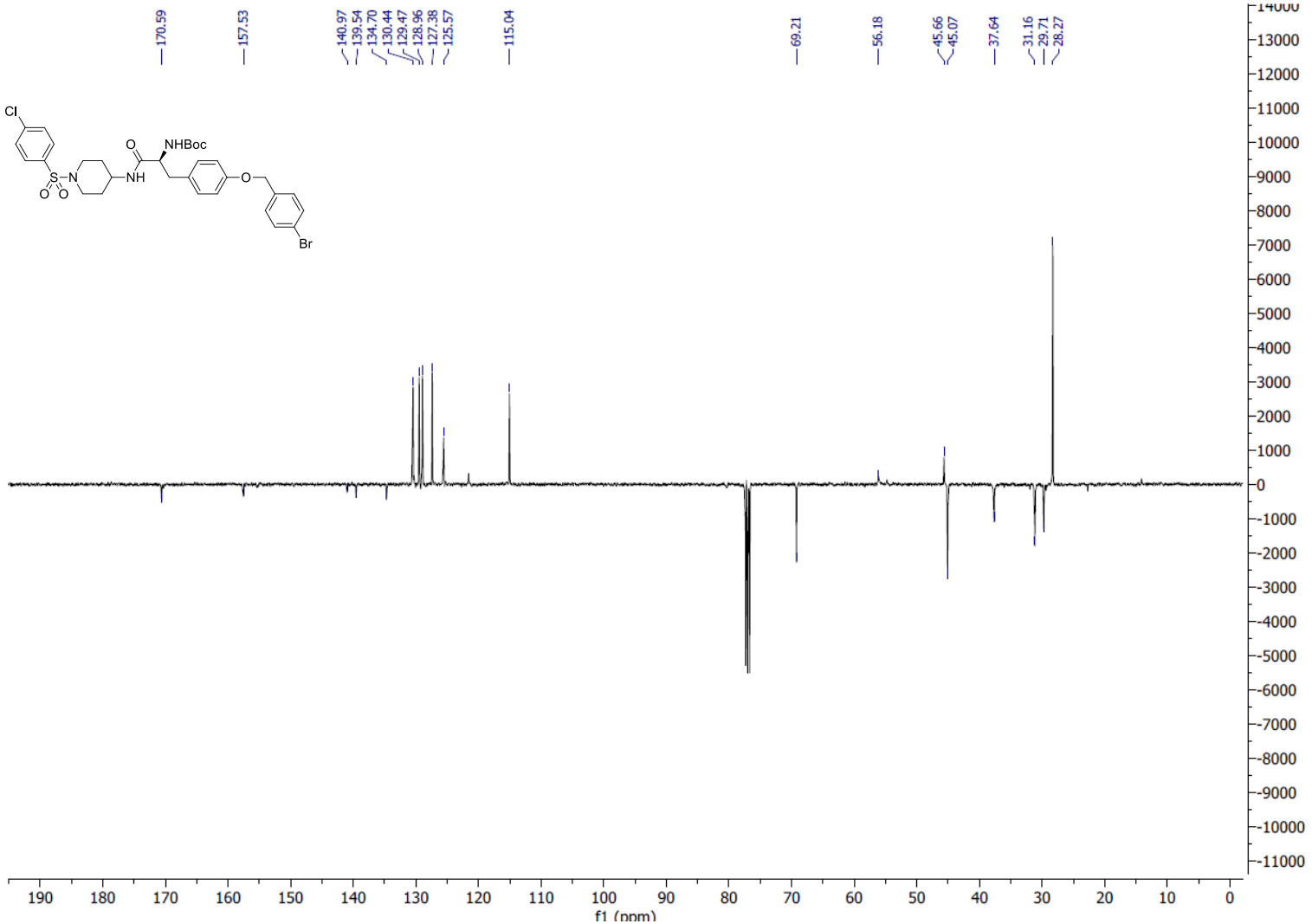

Figure S18: qDEPT NMR spectra for compound **CPK10**

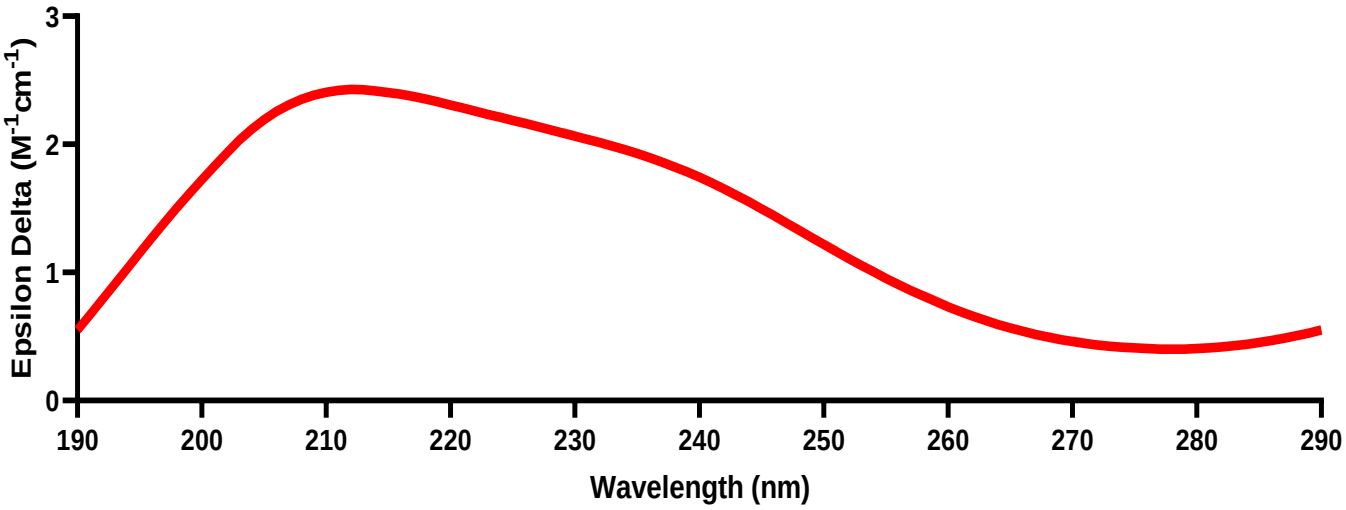

Figure S19: CD spectra for compound **CPK10**

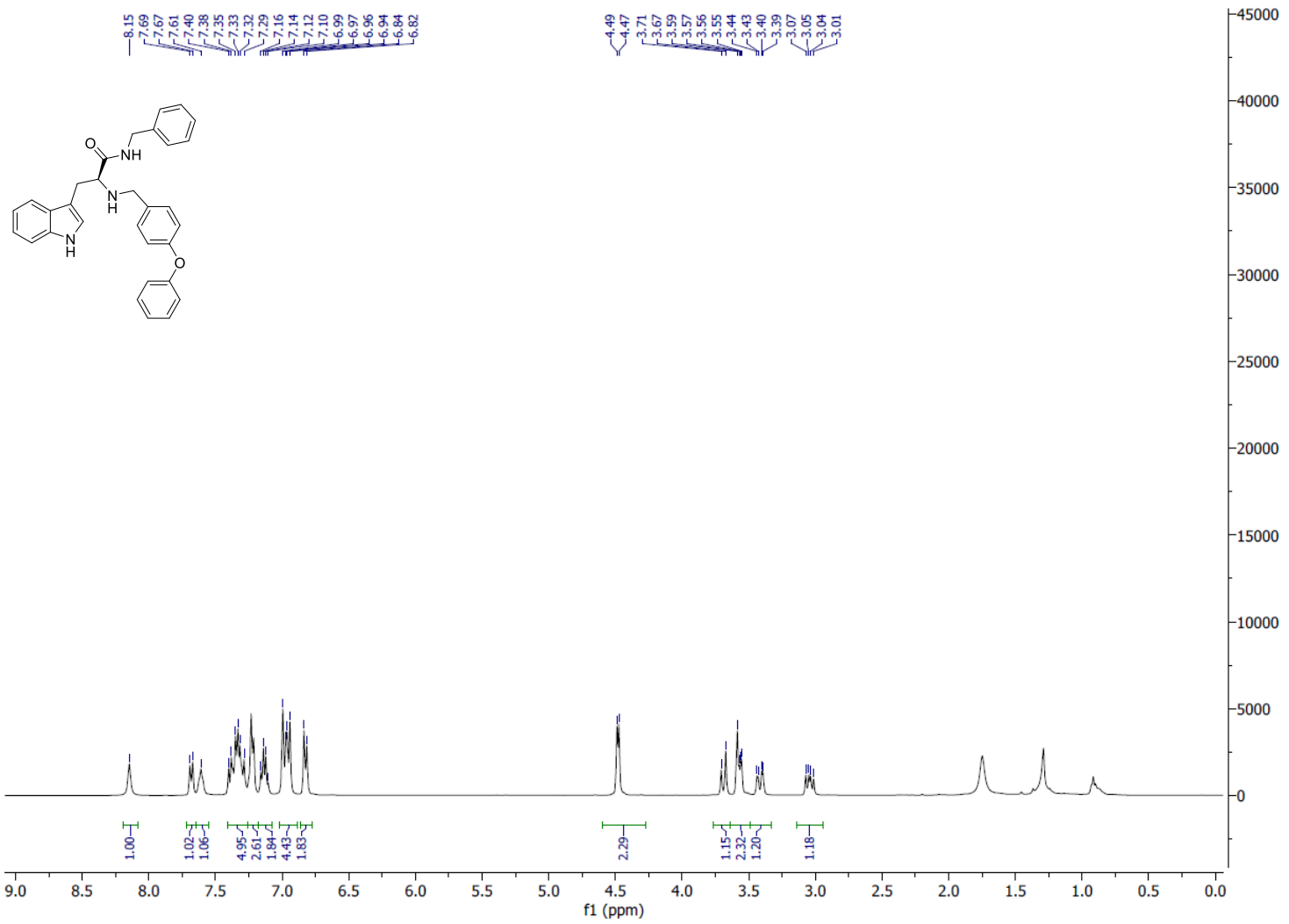

Figure S20: ^{1}H NMR spectra for compound **CPK18**

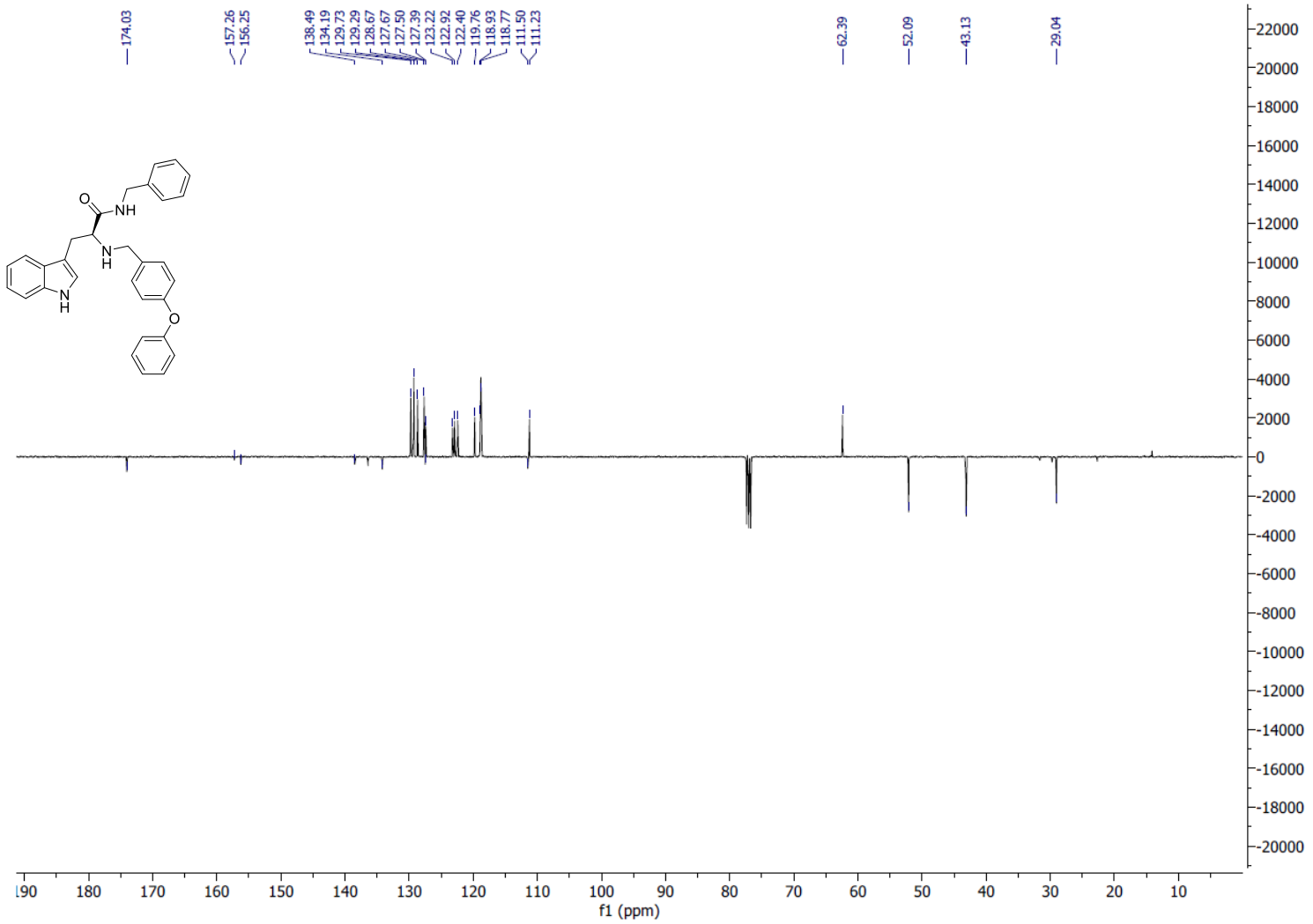

Figure S21: qDEPT NMR spectra for compound **CPK18**

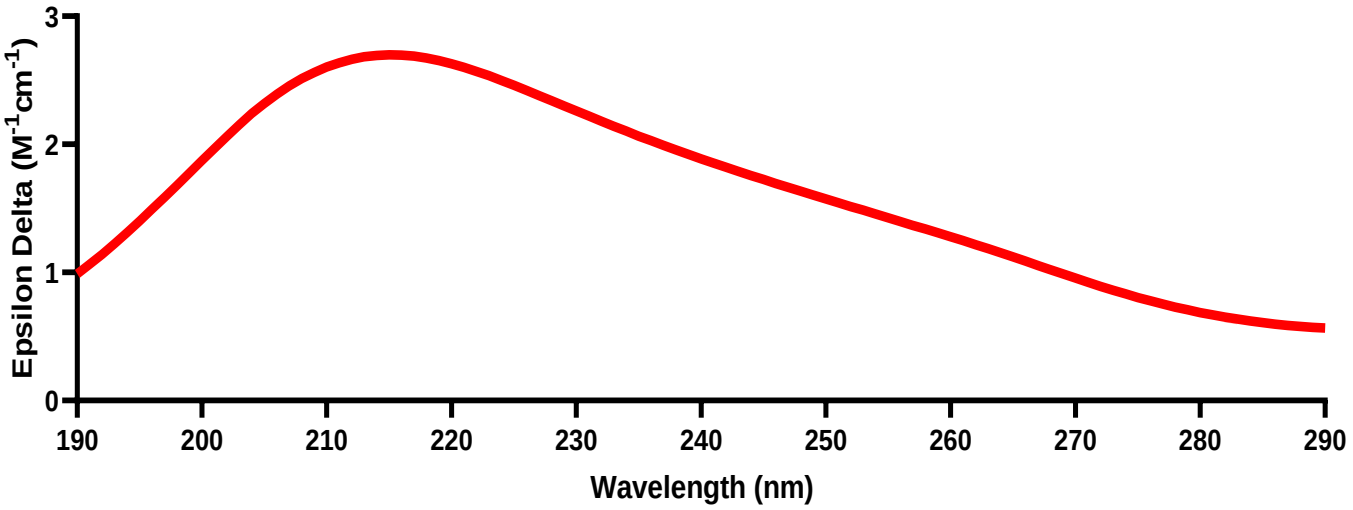

Figure S22: CD spectra for compound **CPK5**

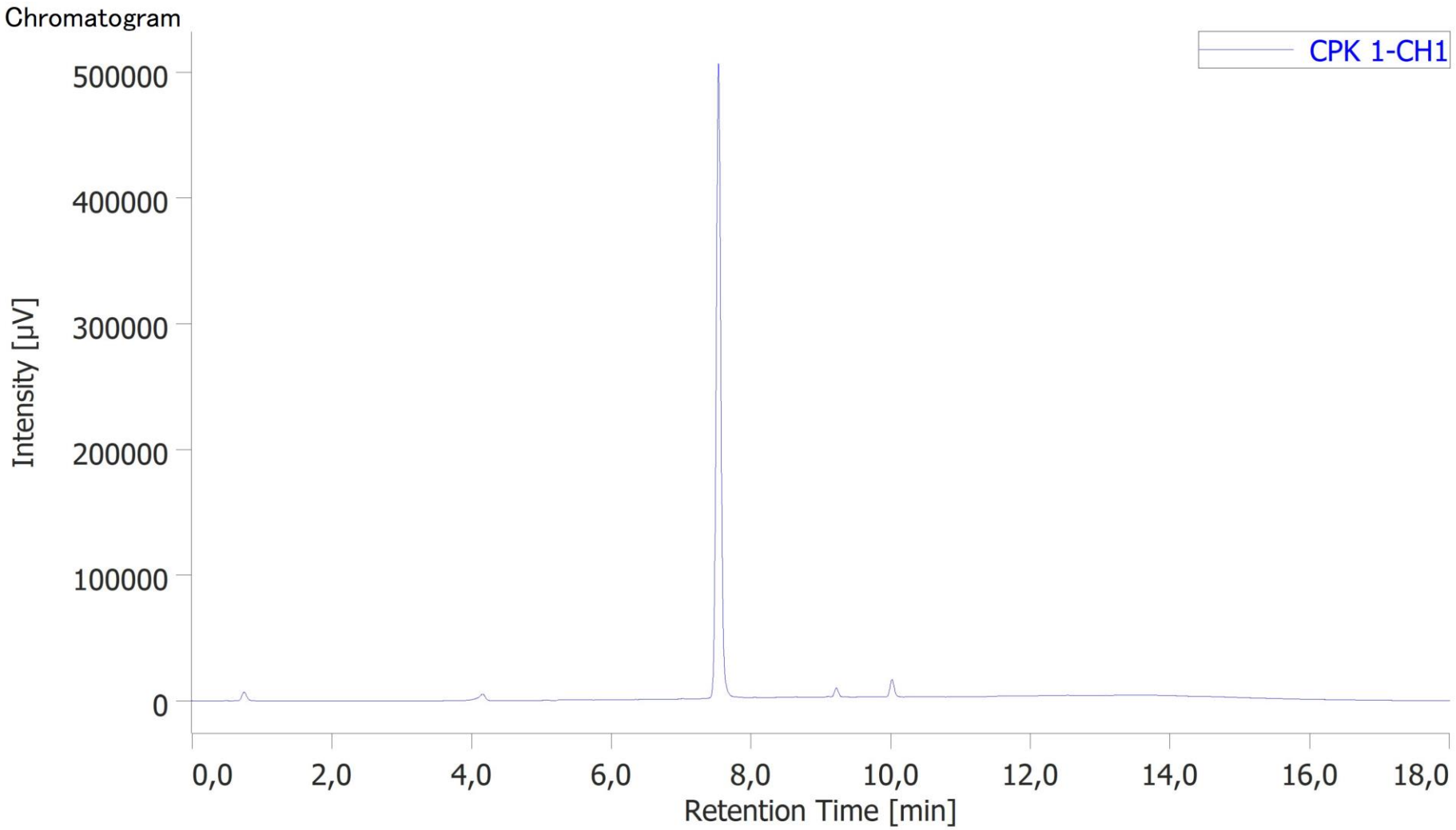

Figures S23: HPLC traces of compound **CPK1**

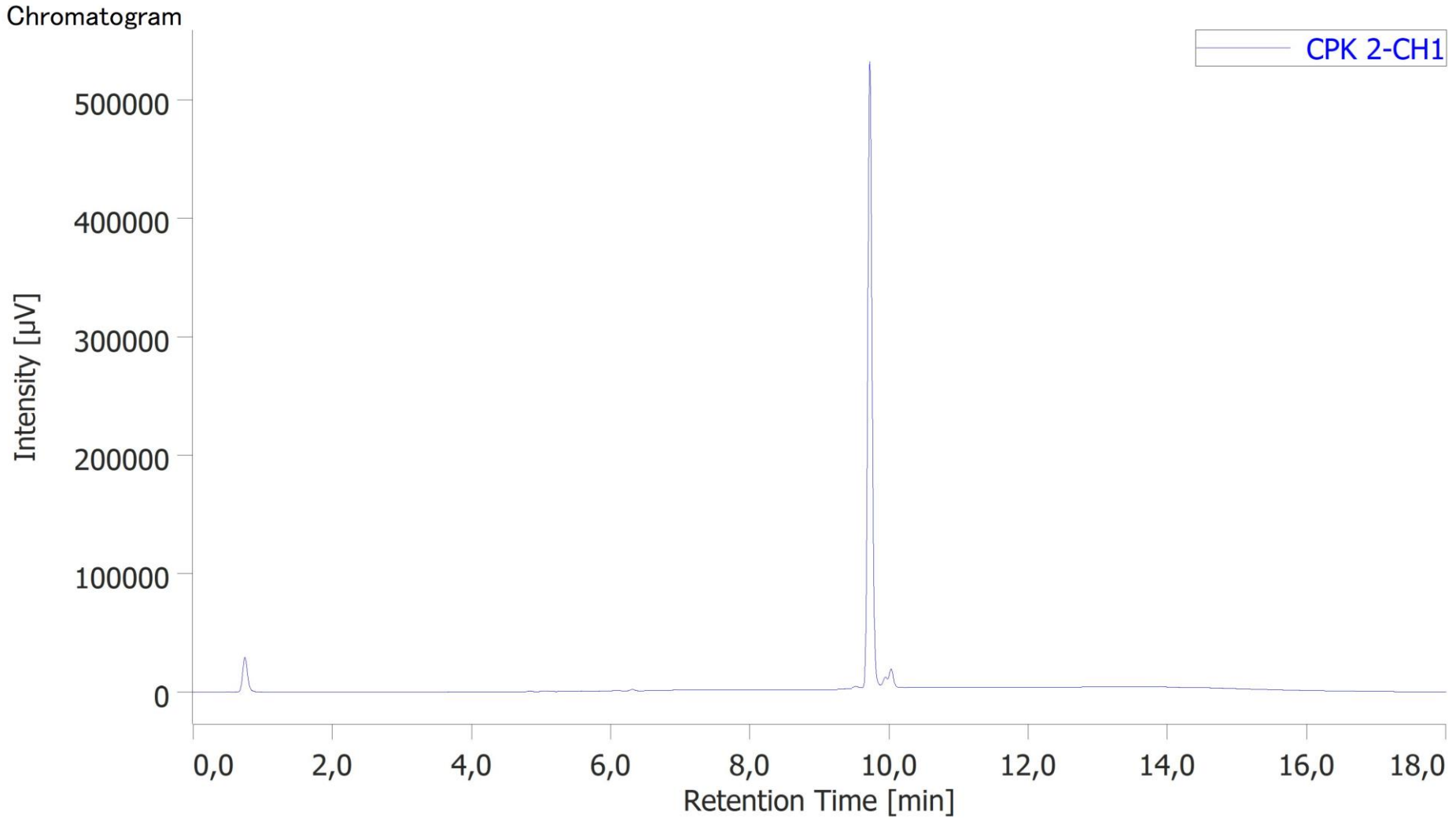

Figures S24: HPLC traces of compound **CPK2**

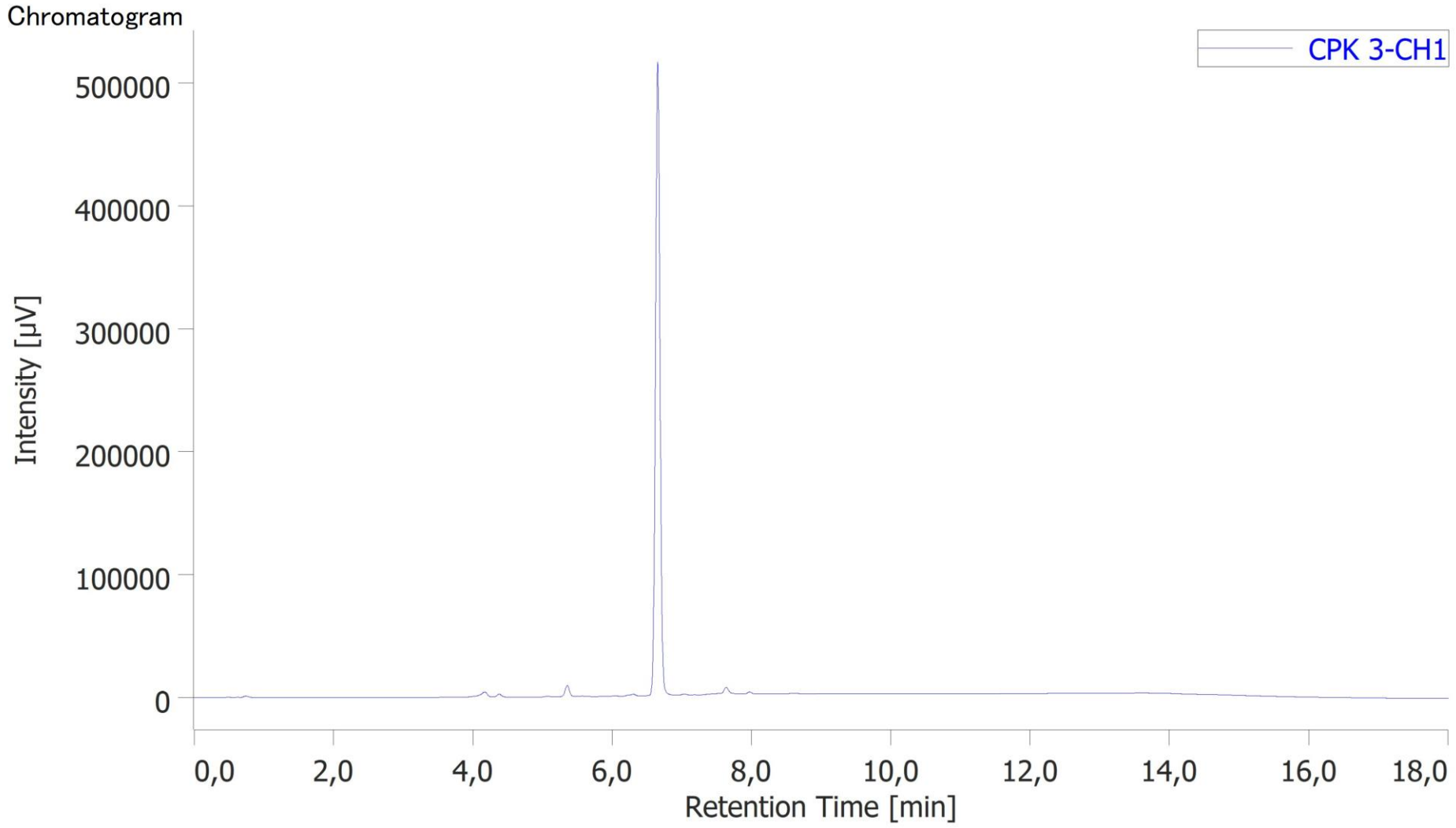

Figures S25: HPLC traces of compound **CPK3**

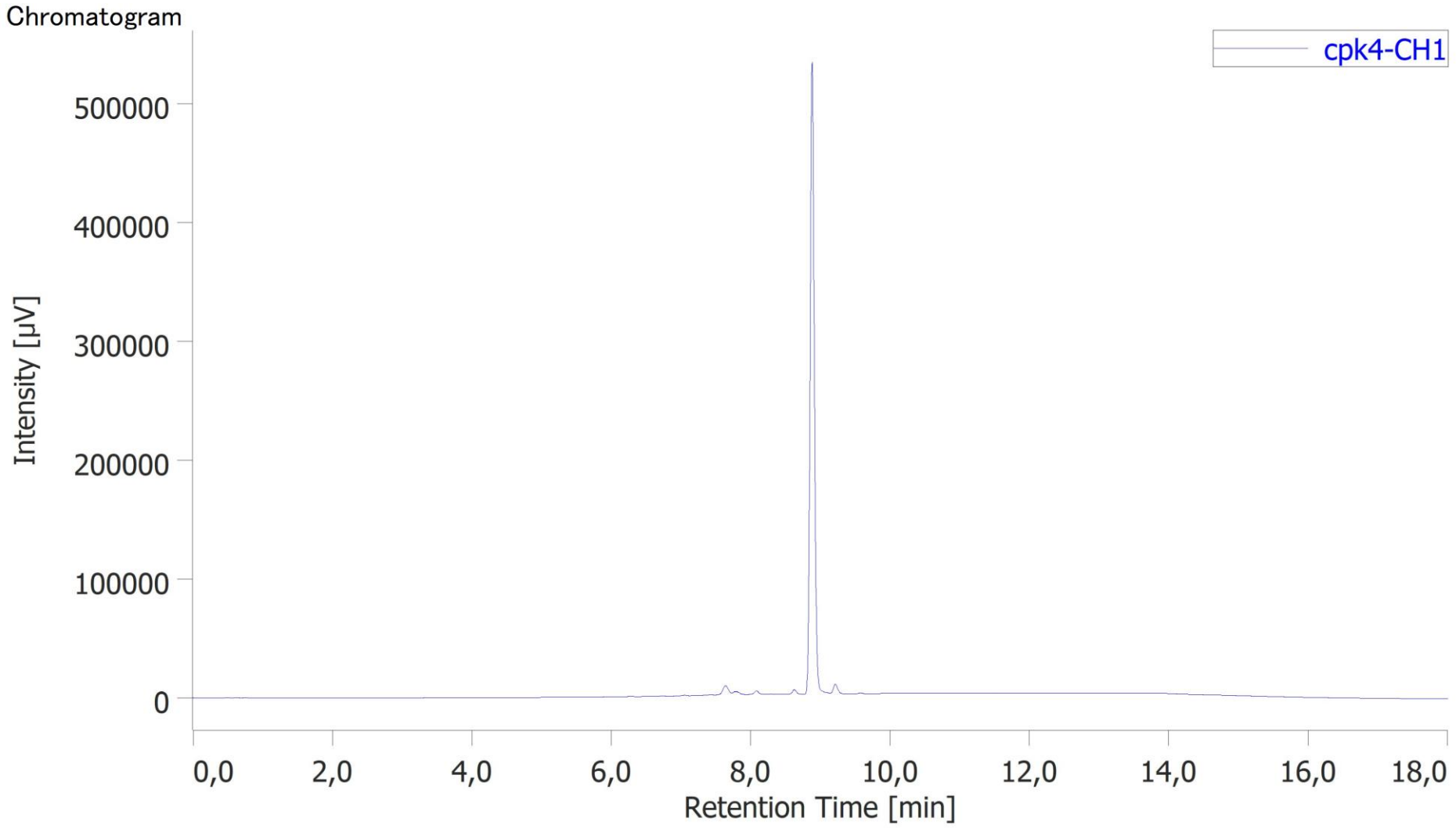

Figures S26: HPLC traces of compound **CPK4**

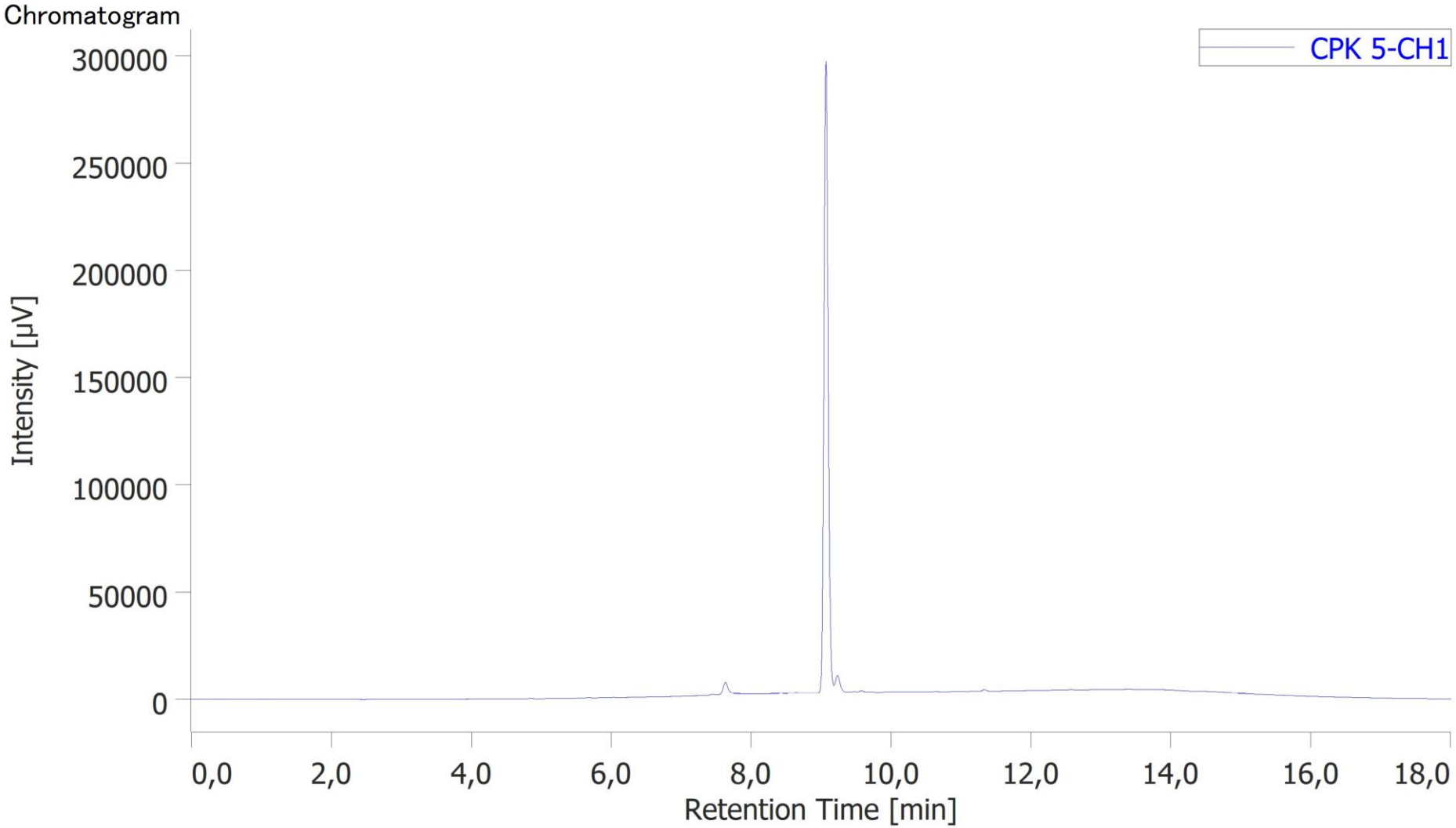

Figures S27: HPLC traces of compound **CPK5**

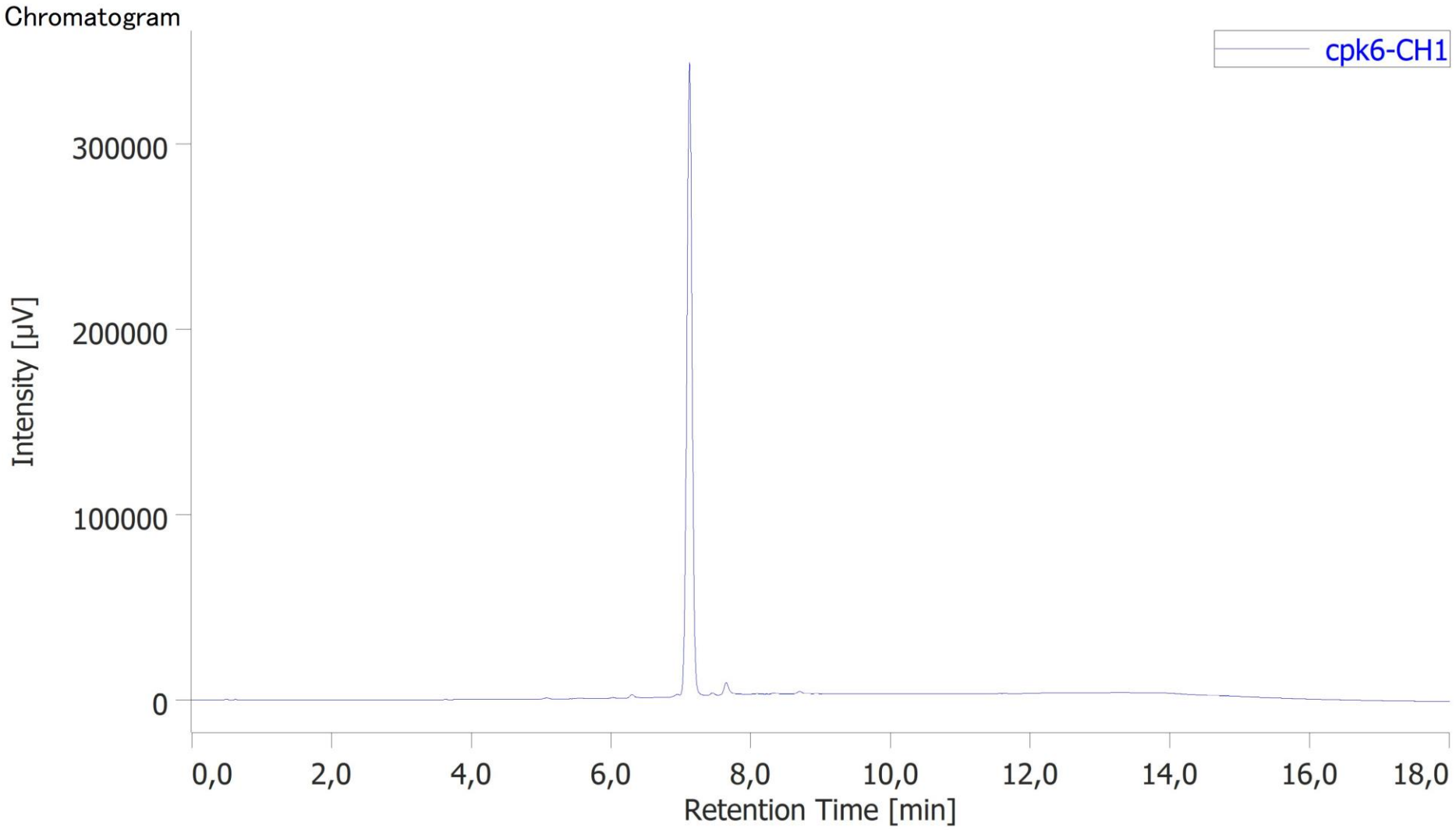

Figures S28: HPLC traces of compound **CPK6**

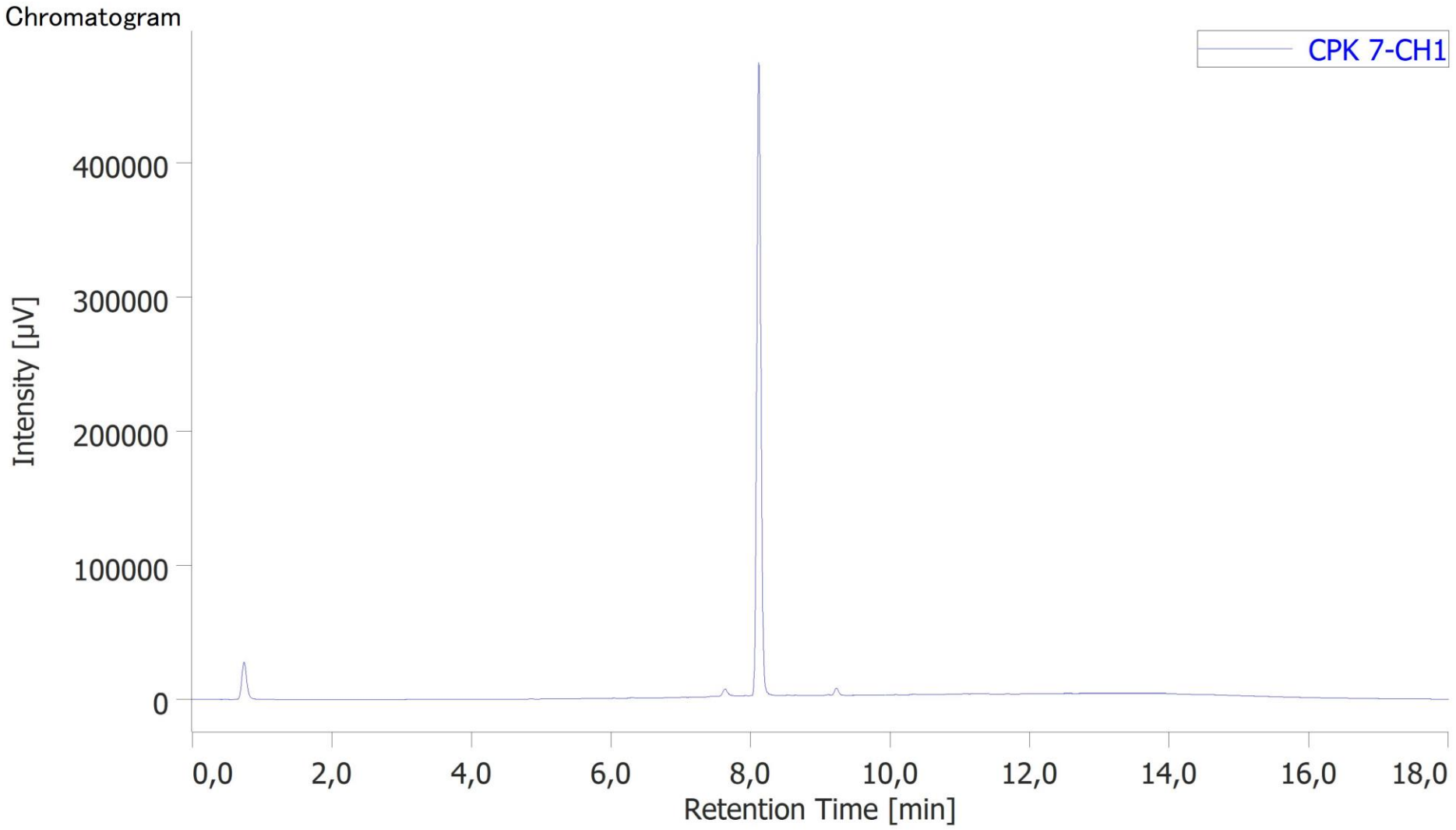

Figures S29: HPLC traces of compound **CPK7**

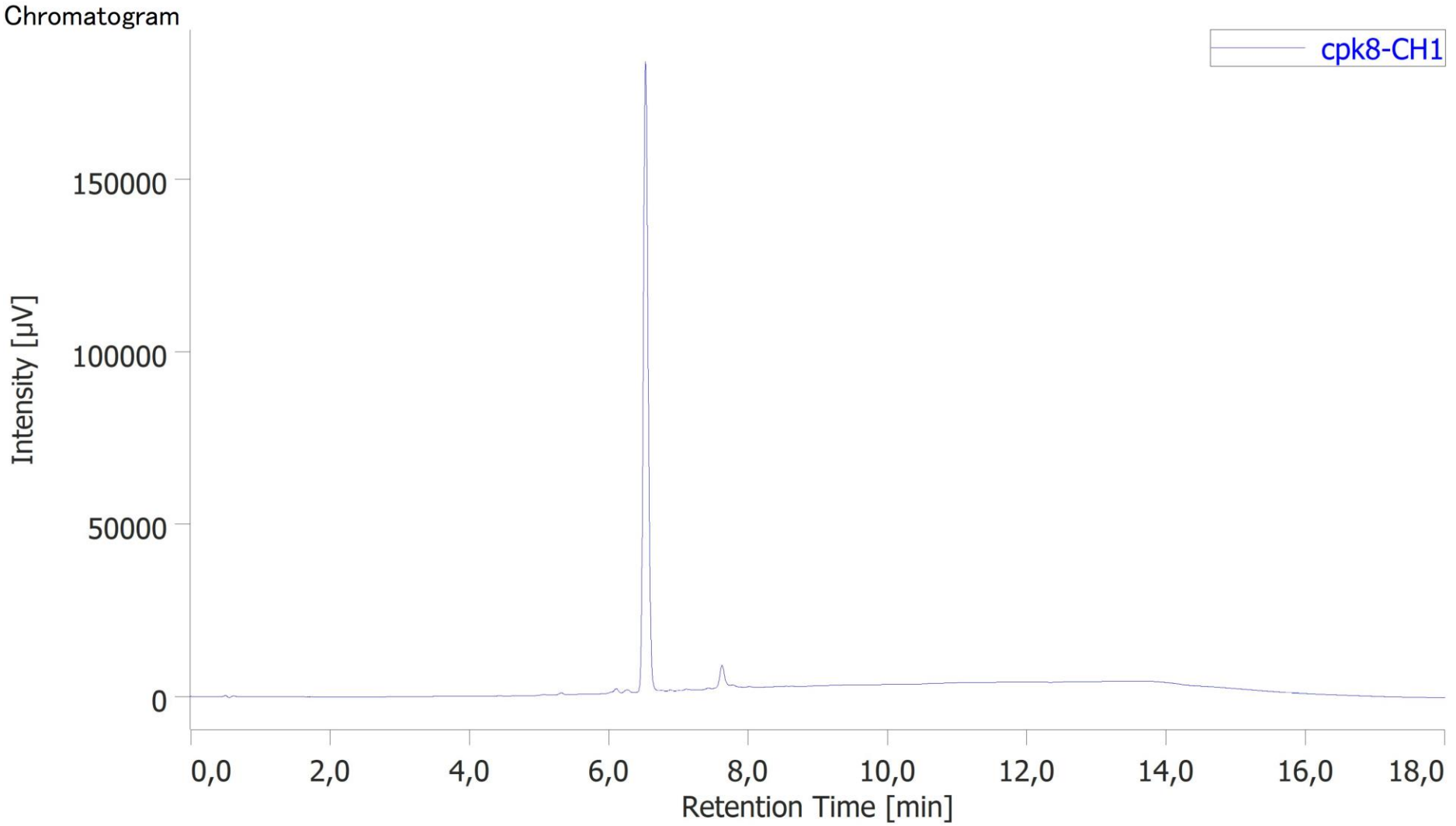

Figures S30: HPLC traces of compound **CPK8**

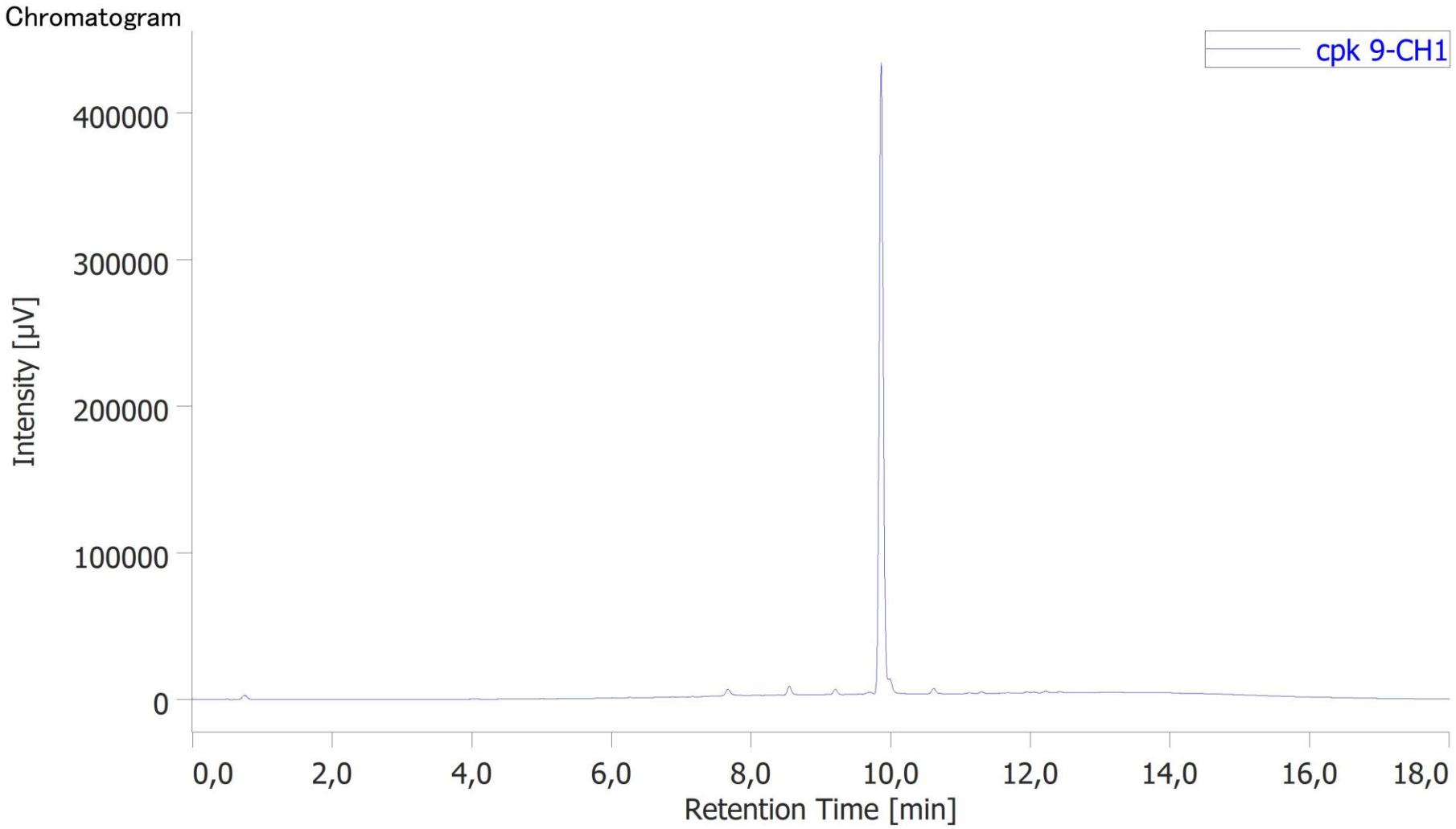

Figures S31: HPLC traces of compound **CPK9**

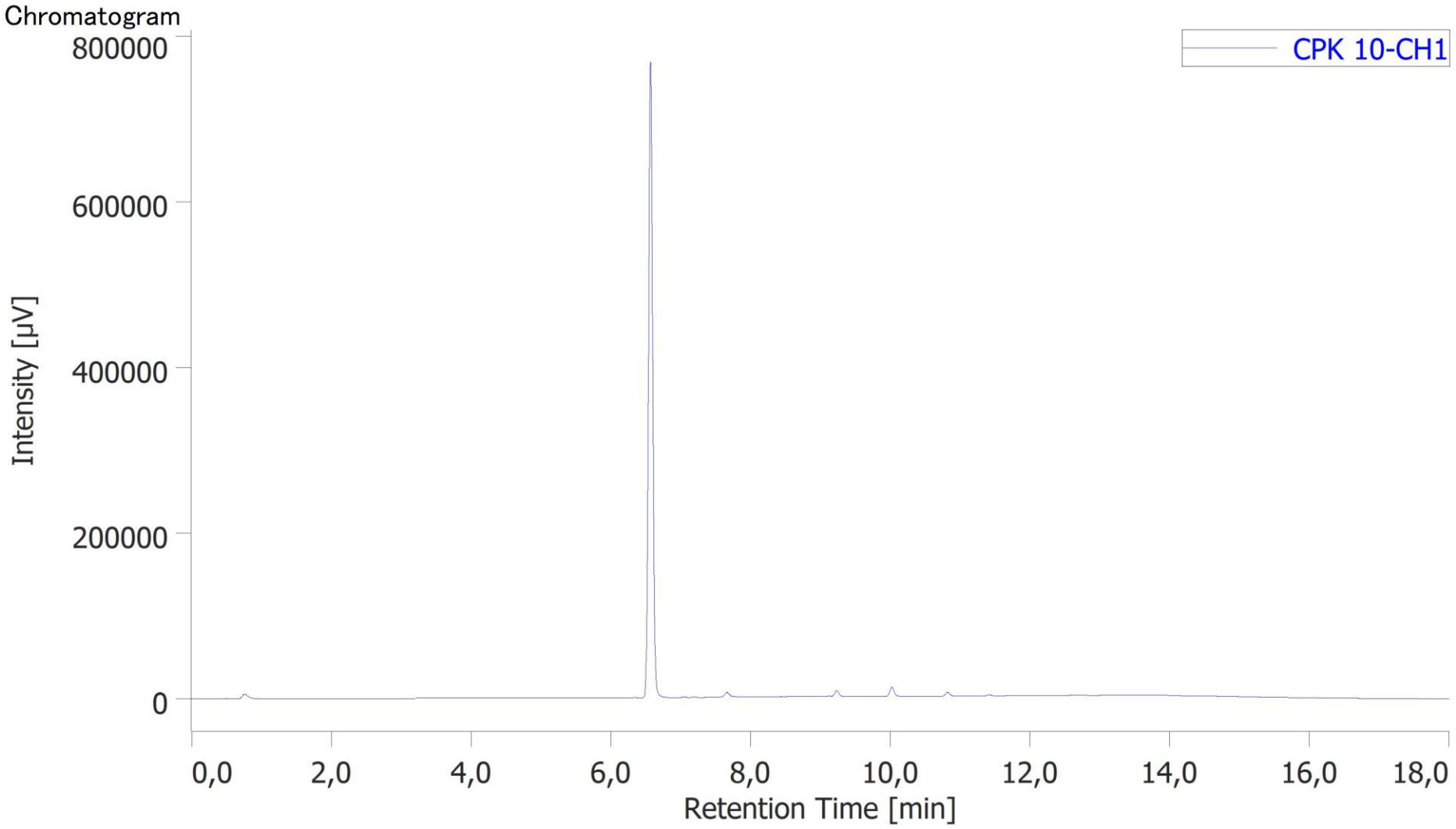

Figures S32: HPLC traces of compound **CPK10**

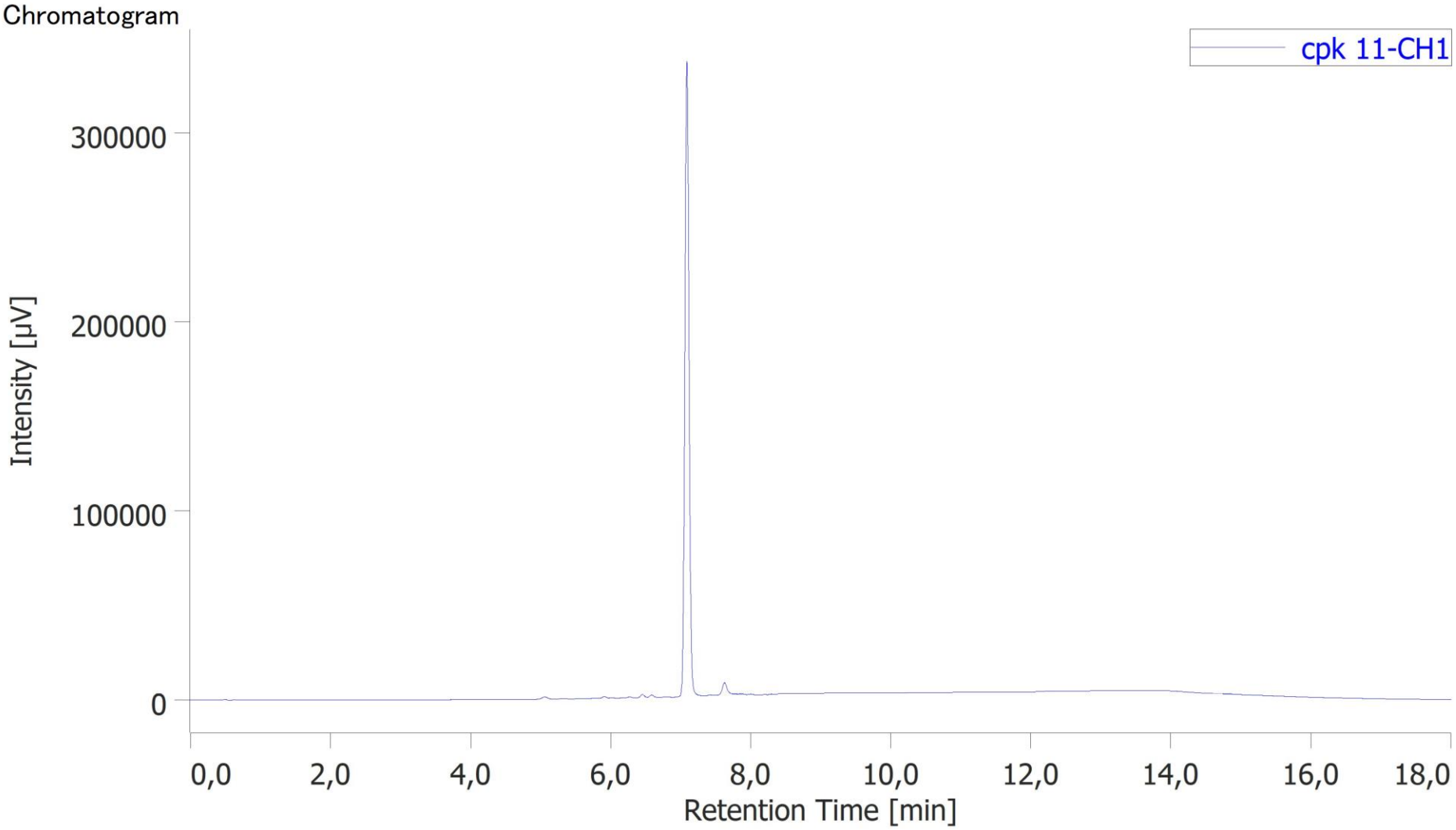

Figures S33: HPLC traces of compound **CPK11**

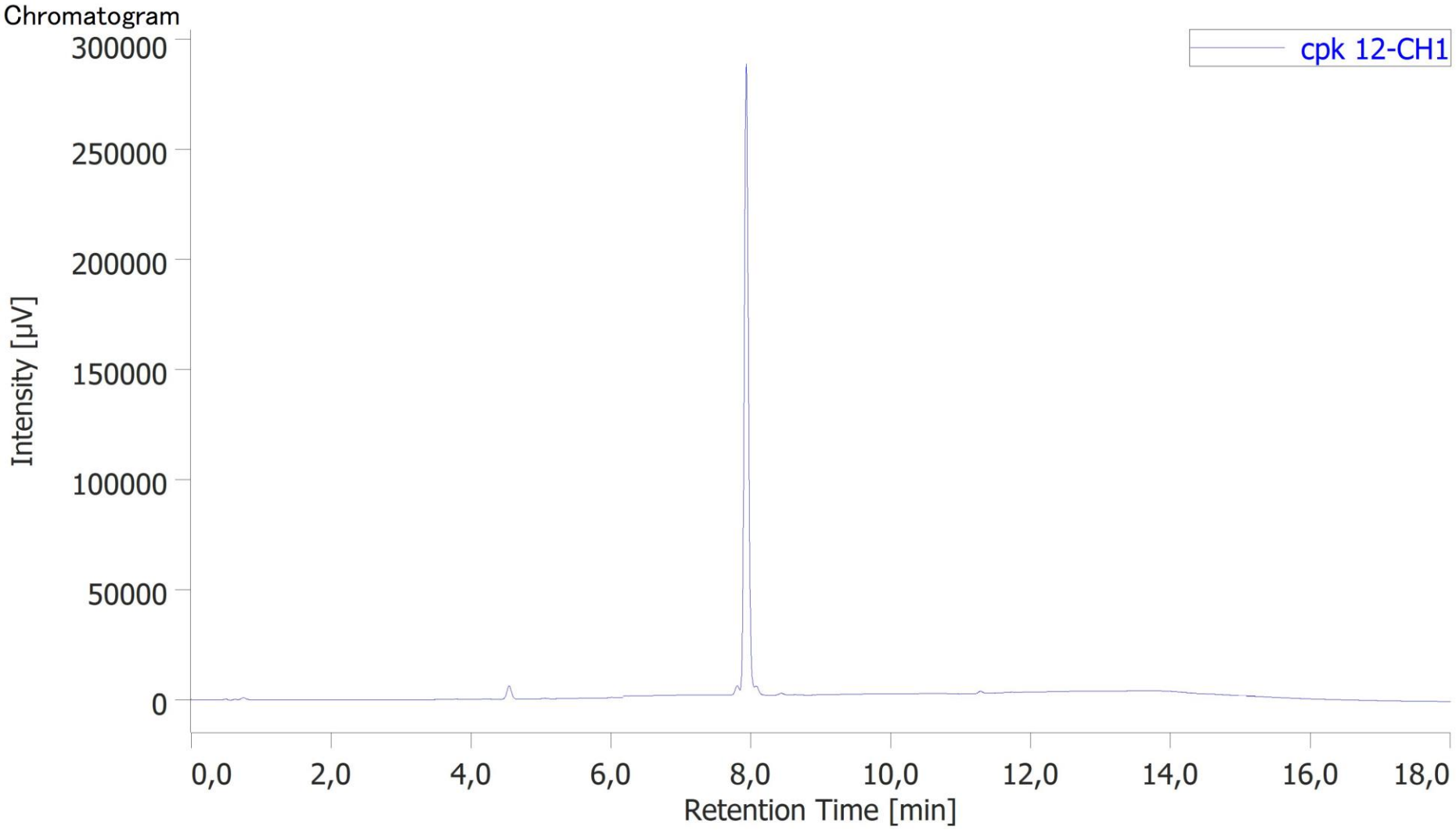

Figures S34: HPLC traces of compound **CPK12**

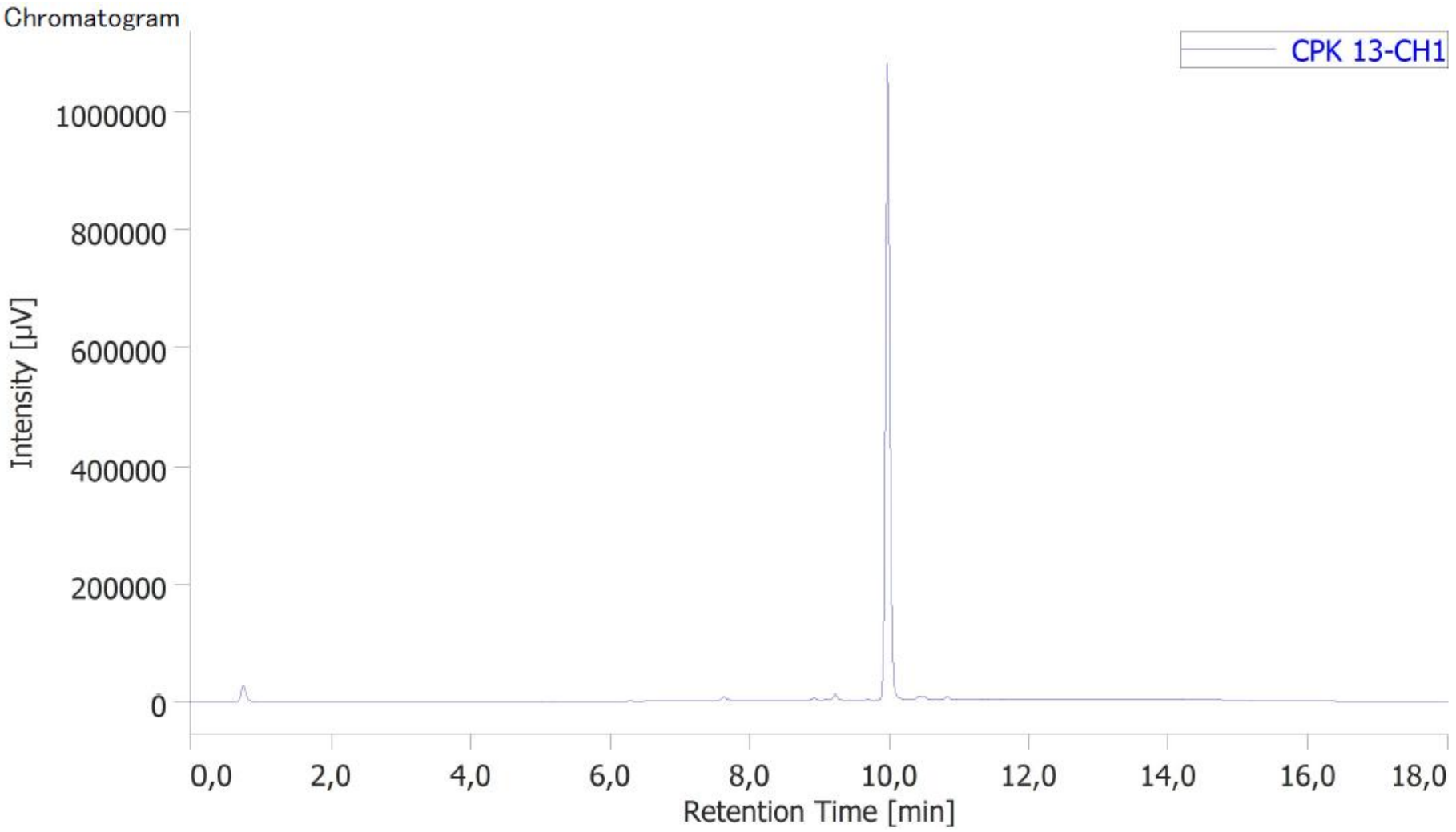

Figures S35: HPLC traces of compound **CPK13**

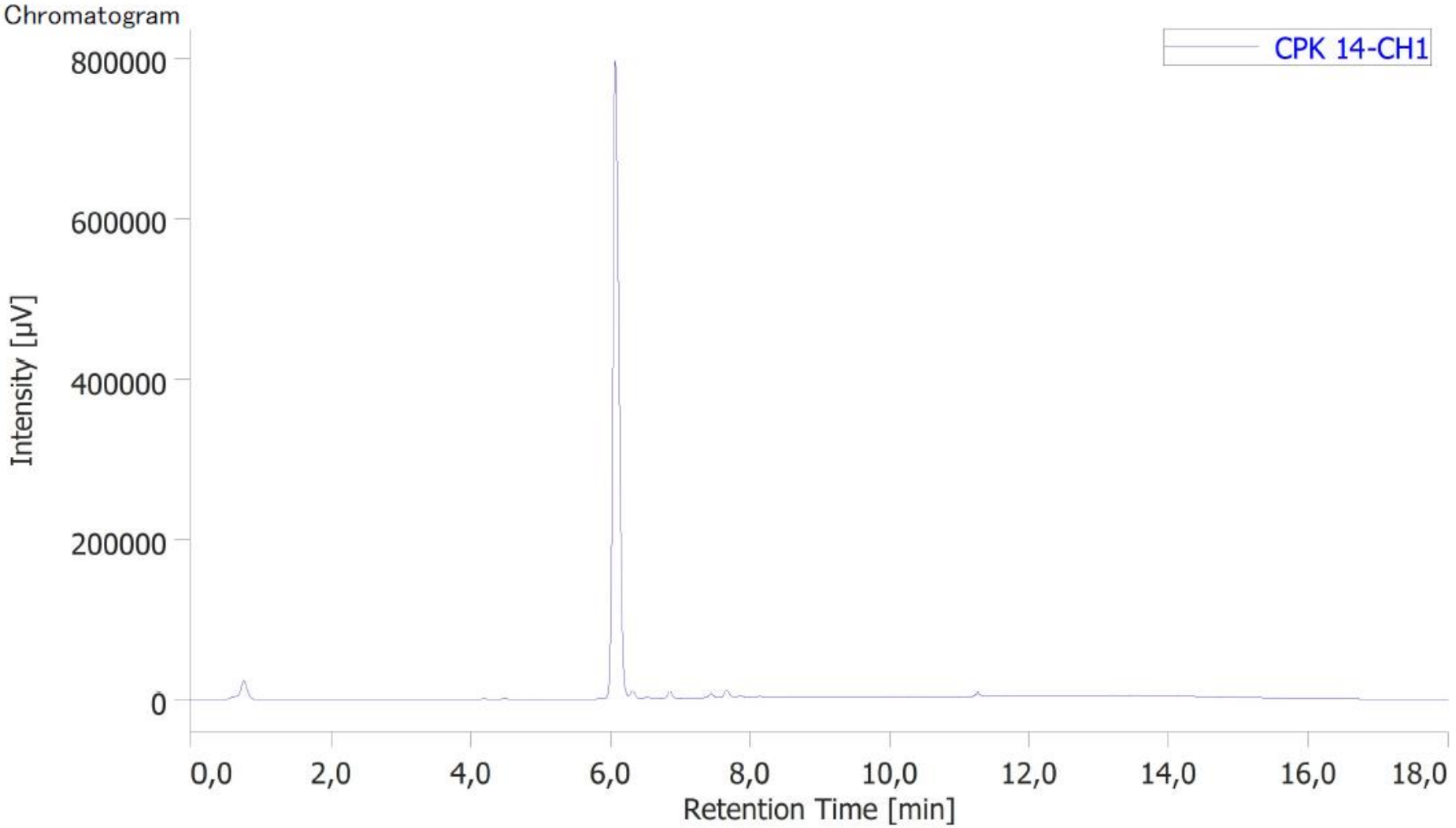

Figures S36: HPLC traces of compound **CPK14**

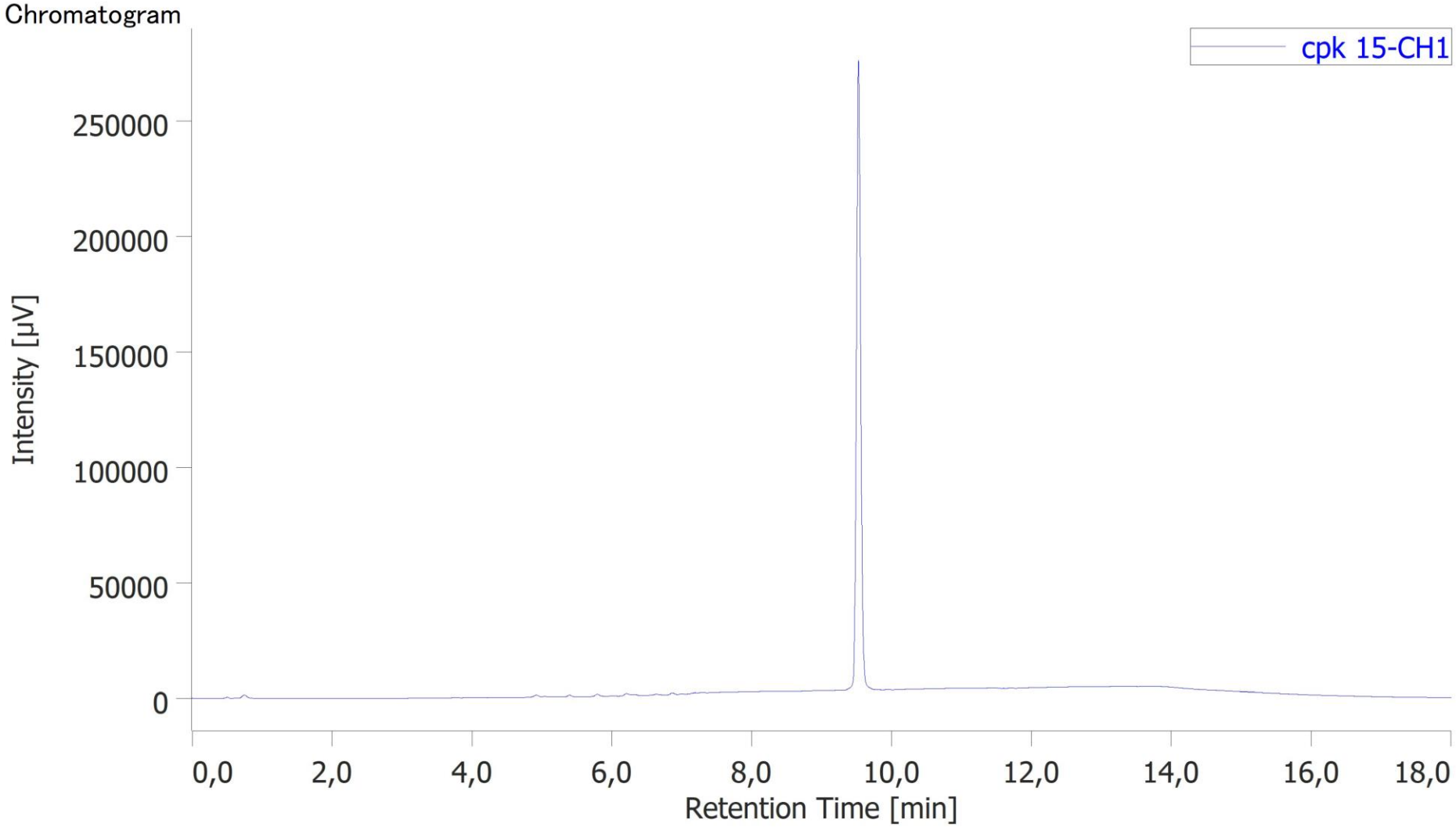

Figures S37: HPLC traces of compound **CPK15**

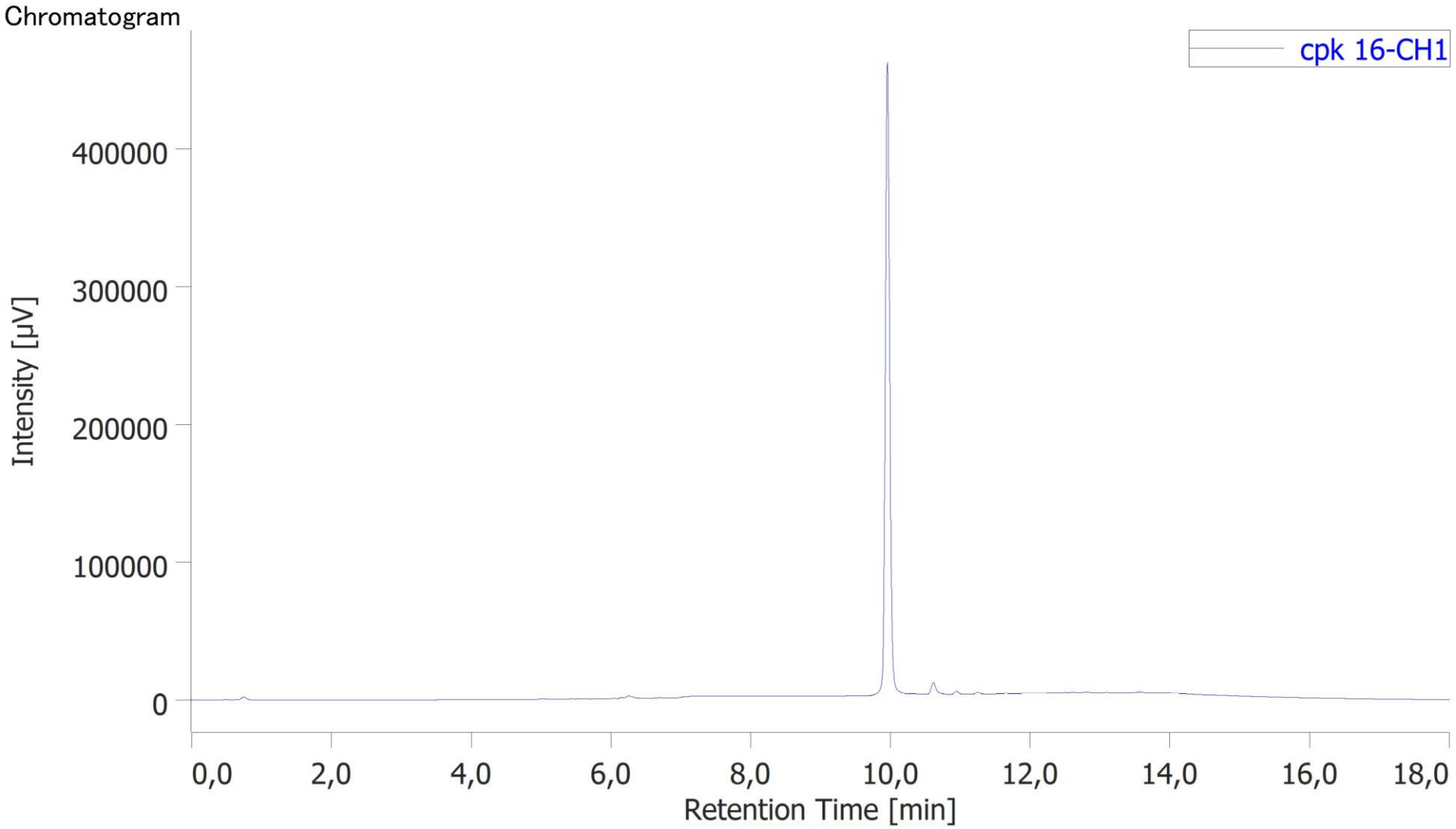

Figures S38: HPLC traces of compound **CPK16**

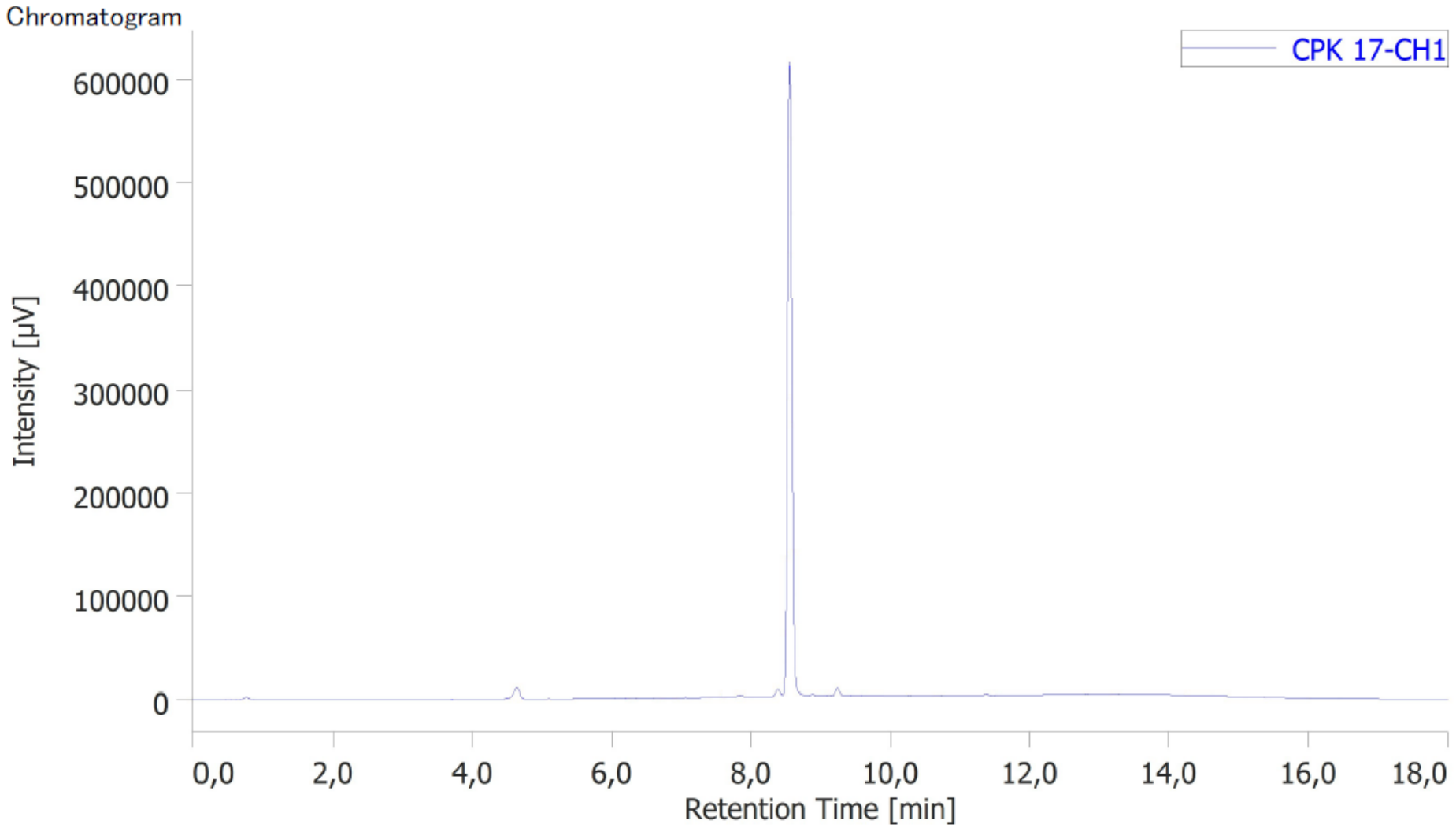

Figures S39: HPLC traces of compound **CPK17**

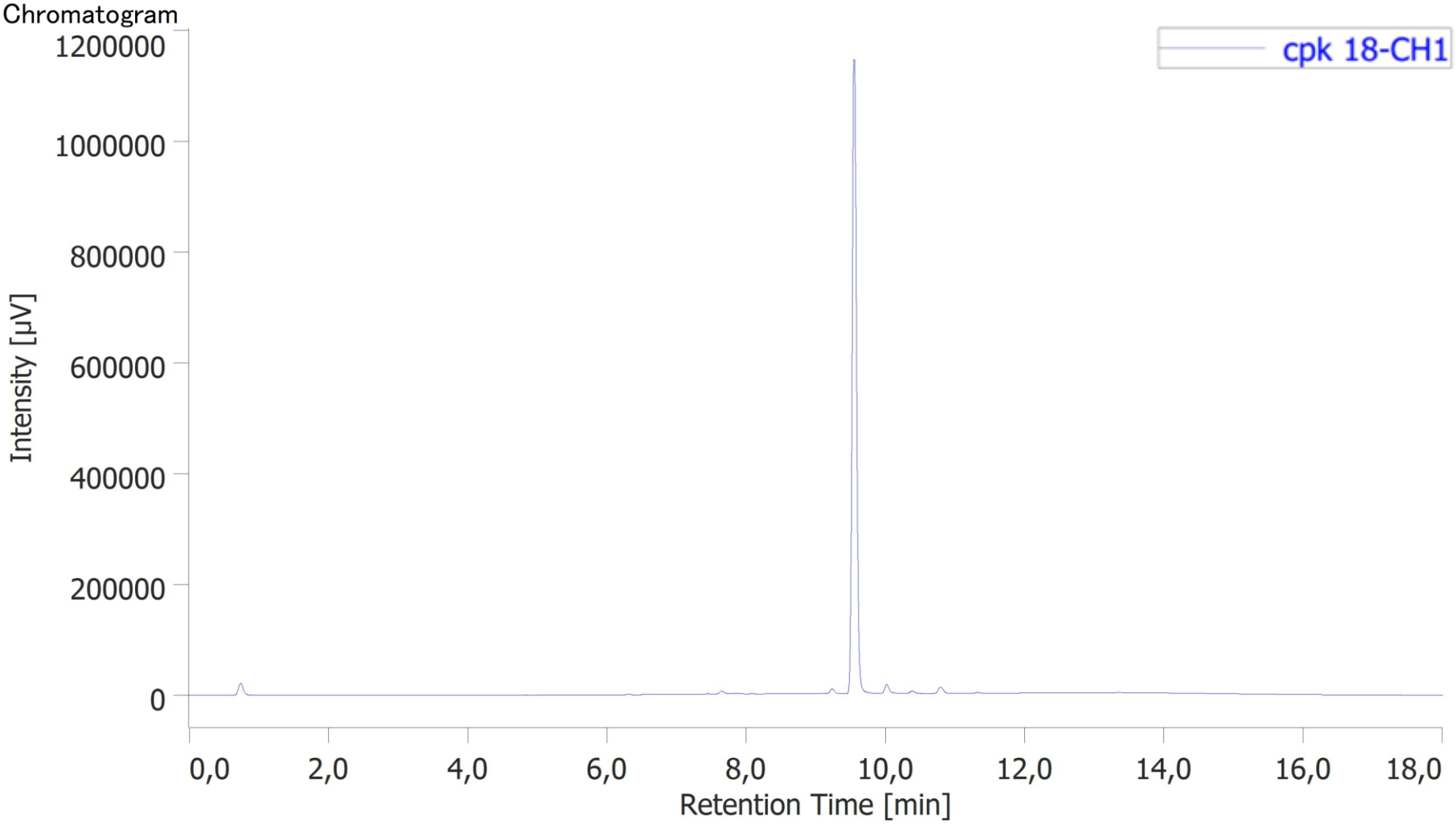

Figures S40: HPLC traces of compound **CPK18**

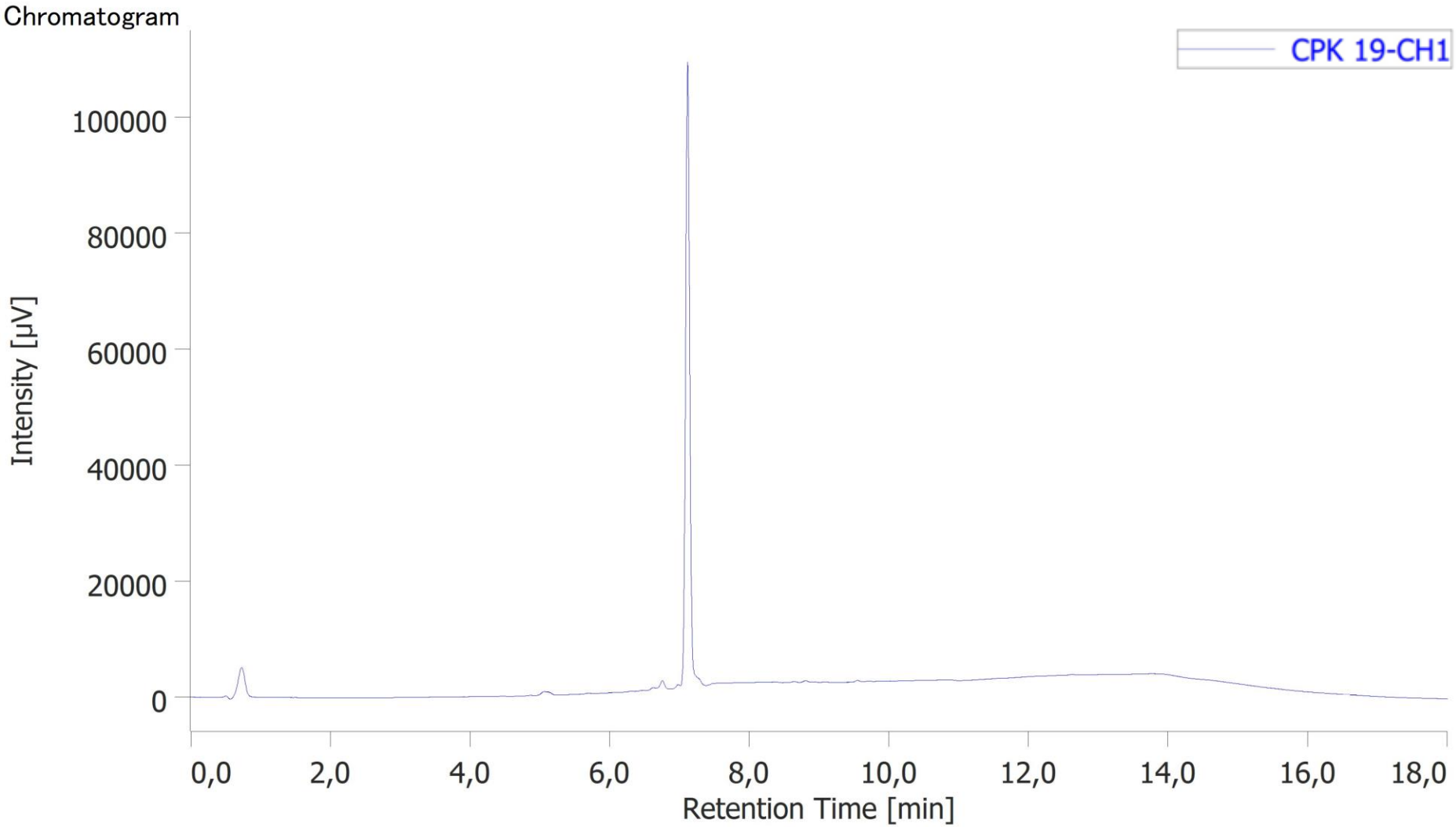

Figures S41: HPLC traces of compound **CPK19**

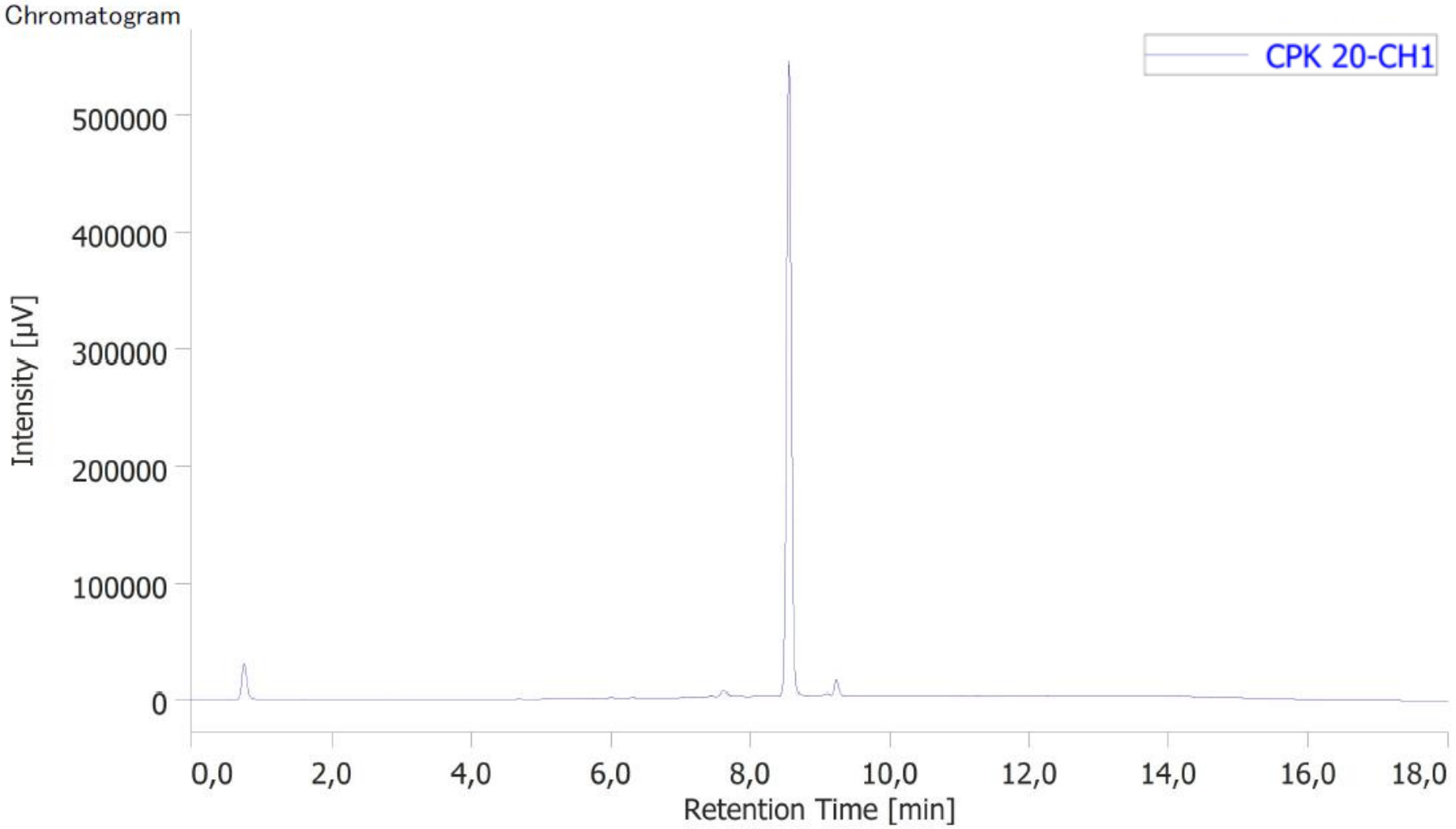

Figures S42: HPLC traces of compound **CPK20**

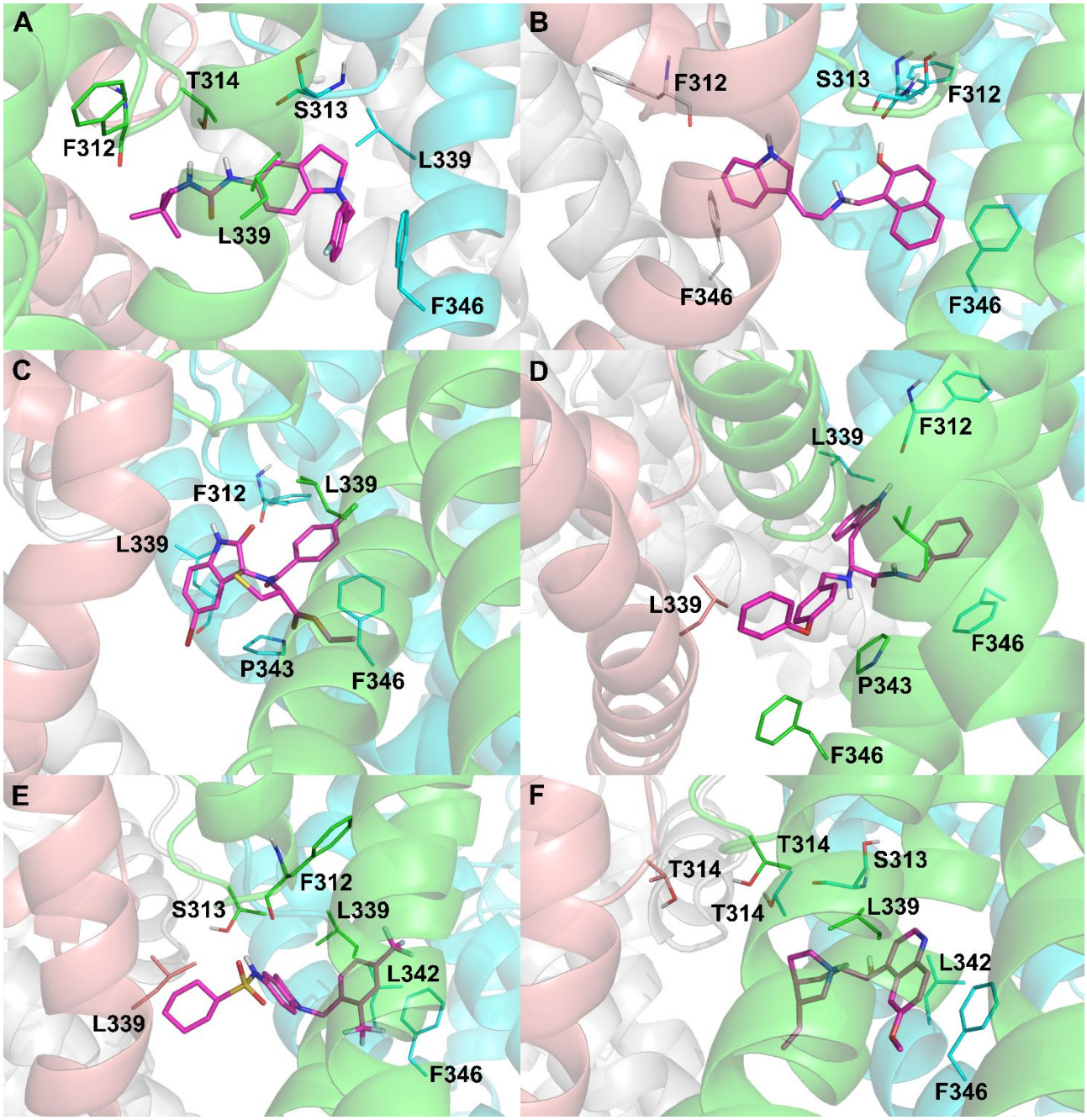

Figure S43: Docking poses of **CPK4 (A)**, **CPK13 (B)**, **CPK16 (C)**, **CPK18 (D)**, **CPK20 (E)** and quinidine **(F)** on HMhKCNT1$_{98\text{-}354}$. In every panel, the ligand is depicted in magenta sticks and hKCNT1 monomers are depicted in cyan, green, salmon and white cartoons and sticks.

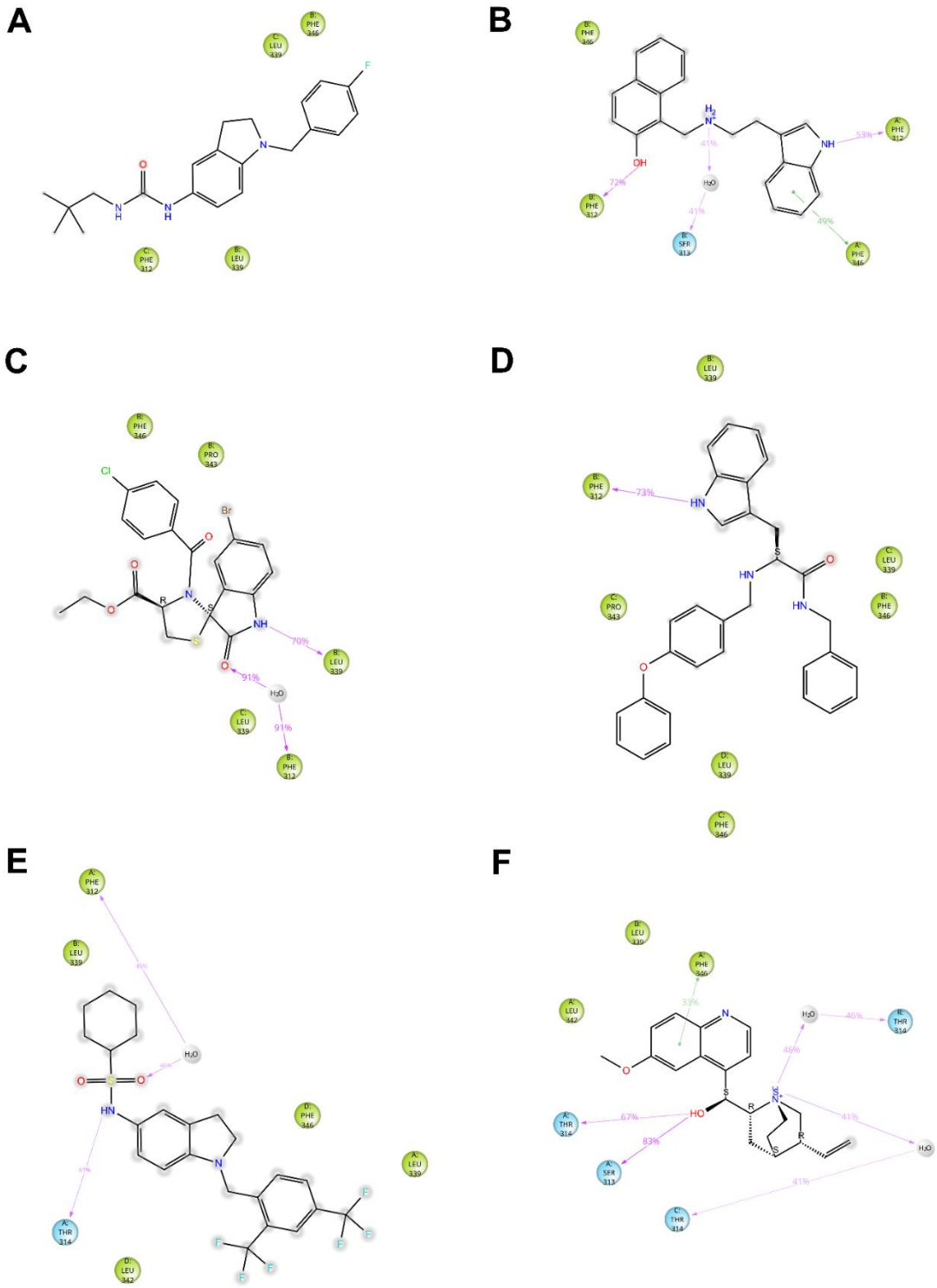

Figure S44: Ligand interaction diagrams of **CPK4 (A)**, **CPK13 (B)**, **CPK16 (C)**, **CPK18 (D)**, **CPK20 (E)** and quinidine **(F)** in complex with HMhKCNT1$_{98\text{-}354}$. Only residues interacting with the ligand for at least 36ns out 120ns of MD simulation are shown. Residues are colored according to the following scheme: cyan - polar; green - hydrophobic; grey - water molecule. Grey halos highlight solvent exposure. H-bonds are represented by magenta arrows (dashed when sidechain atoms are involved, solid in the case of backbone atoms involvement); green solid lines represent π-π stacking interactions.

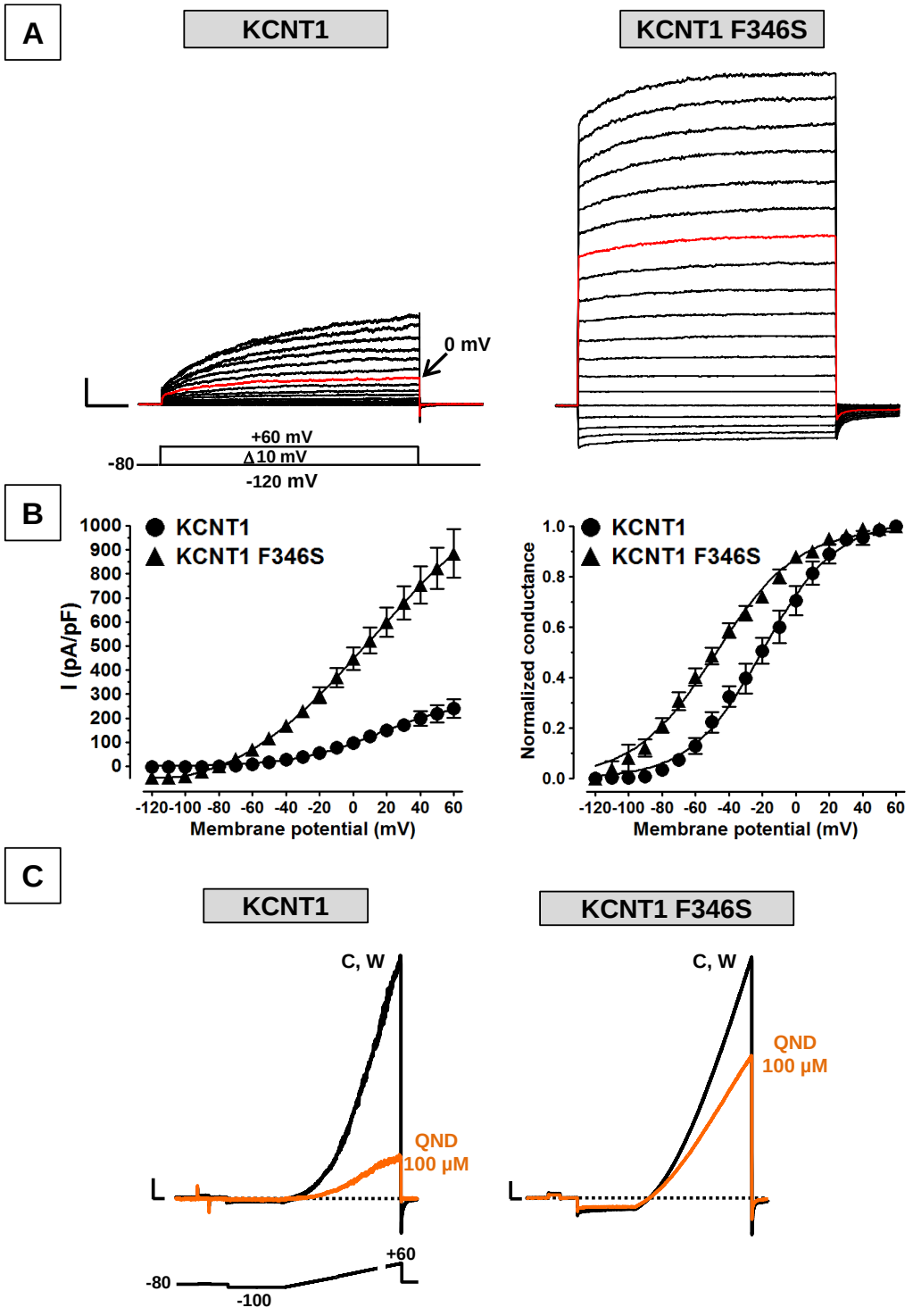

Figure S45: Functional and pharmacological properties of KCNT1 F346S channels. (A) Representative whole-cell currents traces recorded from CHO cells expressing wild-type or mutant homomeric KCNT1 channels, as indicated, in response to the voltage protocol shown below the leftmost traces. Current scale: 1 nA; time scale: 100 ms. (**B**) Current density (left) and normalized conductance (right) of wild-type and mutant KCNT1 channels. (**C**) Representative current traces measured in response to voltage ramps from -100 mV to +60 mV in cells expressing KCNT1 or KCNT1 F346S channels in control solution (C), upon perfusion of 100 µM of quinidine (**QND**), or upon drug washout (W). Current scale: 200 pA for KCNT1, 1 nA for KCNT1 F346S; time scale: 100 ms.

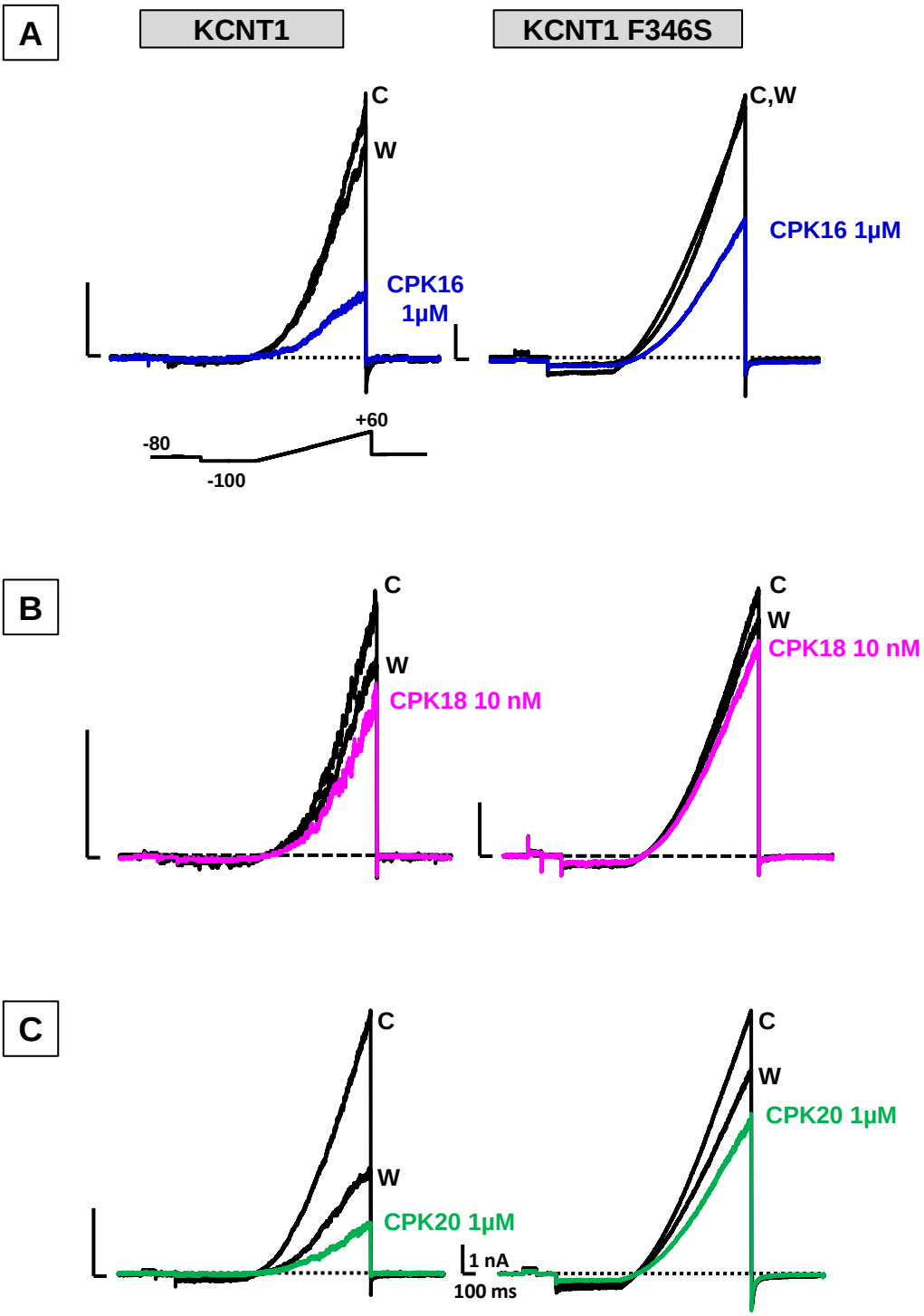

Figure S46: Pharmacological characterization of selected CPK compounds on KCNT1 or KCNT1 F346S channels. (A-B-C) Representative current traces in response to voltage ramps from -100 mV to +60 mV in cells expressing KCNT1 or KCNT1 F346S channels recorded in control solution (CTL), upon perfusion with **CPK16** (10 µM), **18** (10 nM), or **20** (10 µM), or upon drug washout (W). Current scale: 1 nA; time scale: 100 ms.

Parameters	CPK16	CPK18	CPK20
Retention time (min) ± dev. st. (n = 6)	4.34 ± 0.01	2.88 ± 0.01	2.67 ± 0.01
Linearity range (µM)	0.125-20.0	0.250-20.0	0.06-10.0
Intercept	-0,0332	-0.3627	0.0418
Slope	1.8894	0.1901	0.0822
Correlation coefficient (R^2)	0.9999	0.9992	0.9992
Standard deviation of intercept	0.0352	0.1222	0.0537
Standard deviation of the slope	0.0081	0.0027	0.0010
Standard deviation of residuals	0.0753	0.2407	0.1174
LOD (nM)	8.7	15.4	3.0
LOQ (nM)	26.4	46.6	1.0

Table S2: Method validation parameters for LC/MS quantitation of test compounds.

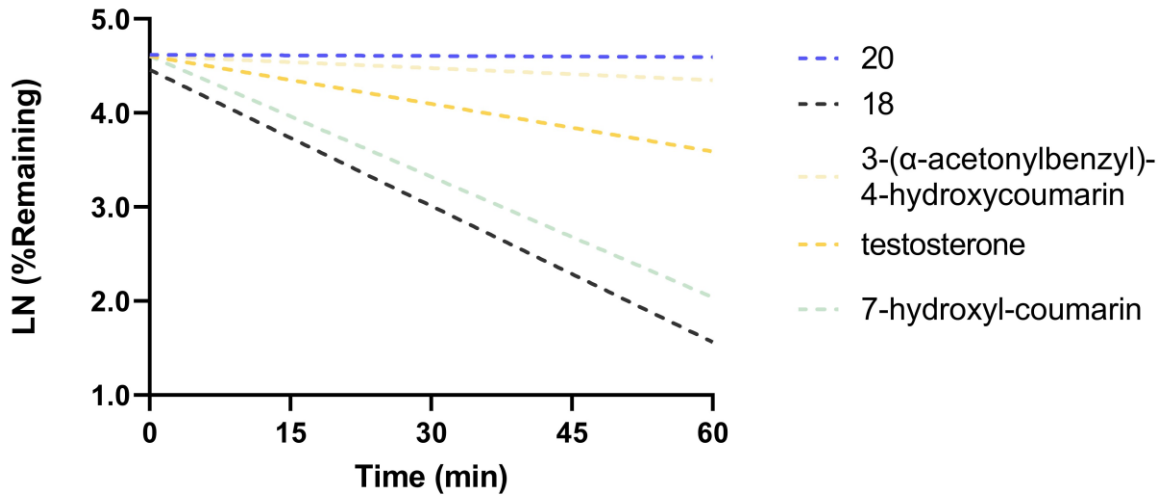

Figure S47: Representative graph showing the linear regression of the natural logarithm of % remaining parent compounds **CPK19** and **CPK20** plotted against incubation time (min). 3-(α-acetonylbenzyl)-4-hydroxycoumarin, testosterone, 7-hydroxyl-coumarin were employed as controls for high, moderate, and low metabolic stability.

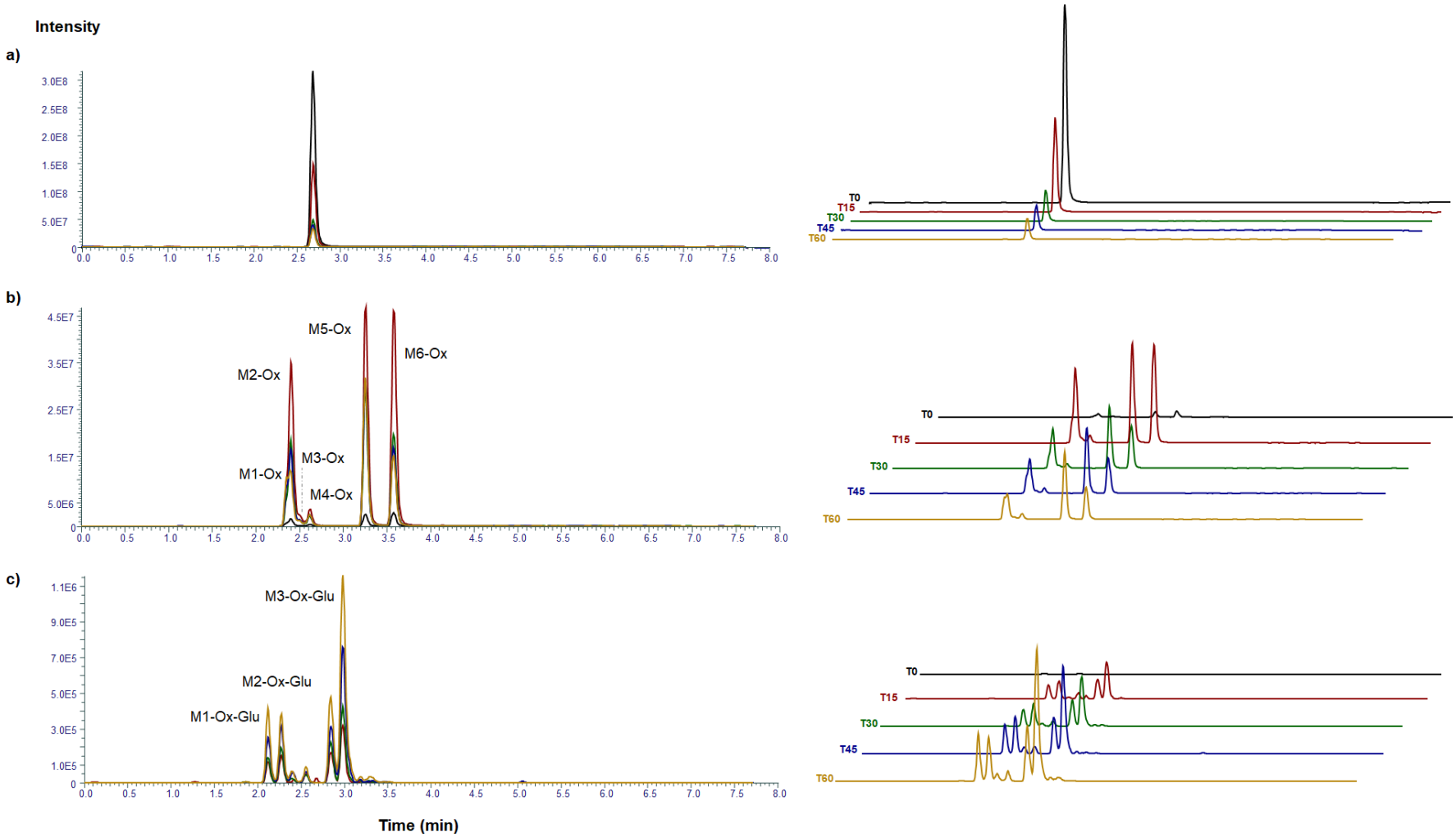

Figure S48: Compound **CPK18** metabolic fate as determined by LC analysis. **(a)** Time course LC traces showing **CPK18** metabolic-dependant decrease in concentration; **(b)** Time course LC trace of the **CPK18** oxidized metabolites; **(c)** Time course LC trace of the main **CPK18** glucuronic metabolites.

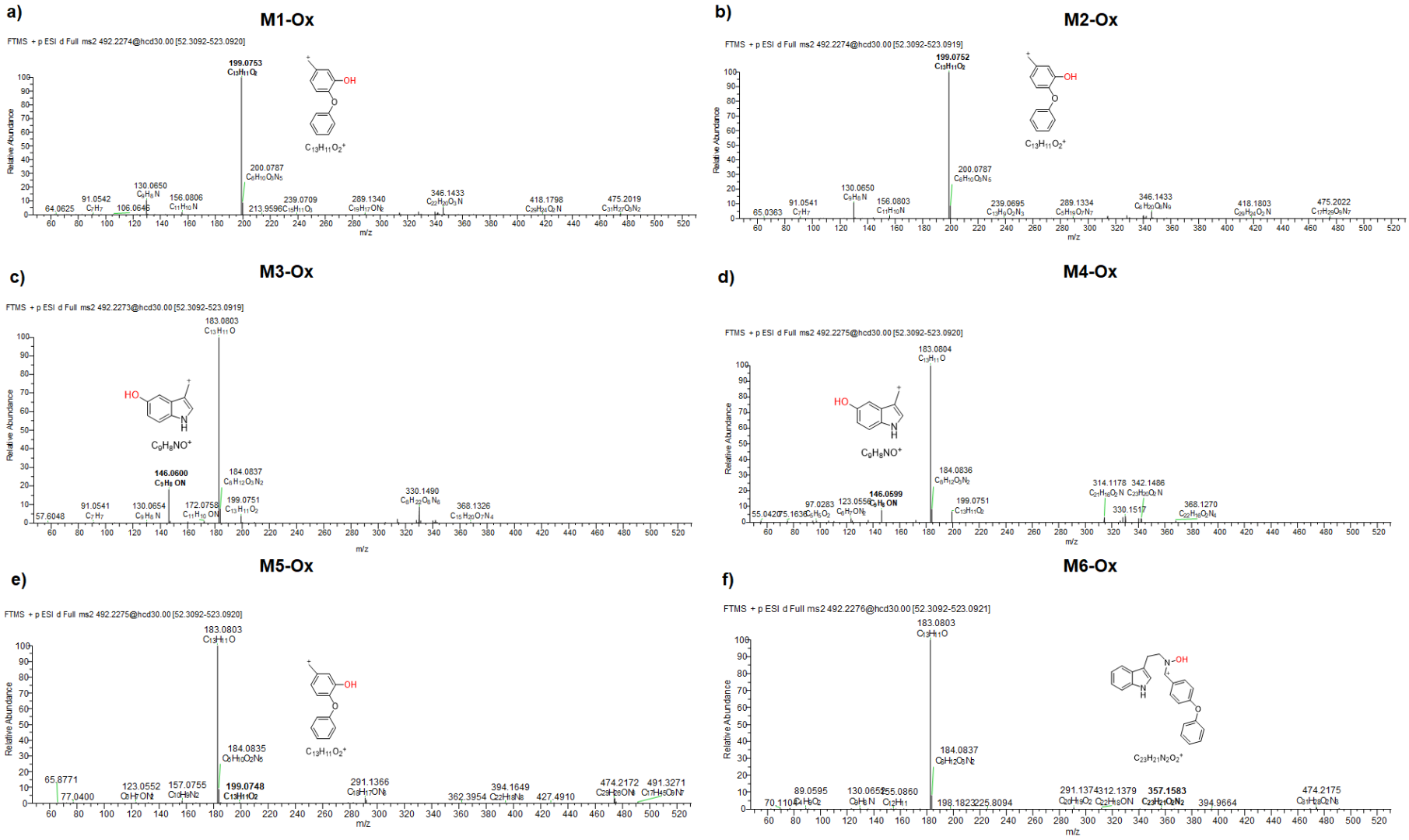

Figure S49: Molecular structures of compound **CPK18** oxidized metabolites M1-Ox **(a)**, M2-Ox **(b)**, M3-Ox **(c)**, M4-Ox **(d)**, M5-Ox **(e)** and M6-Ox **(f)** as determined by MS/MS analysis.

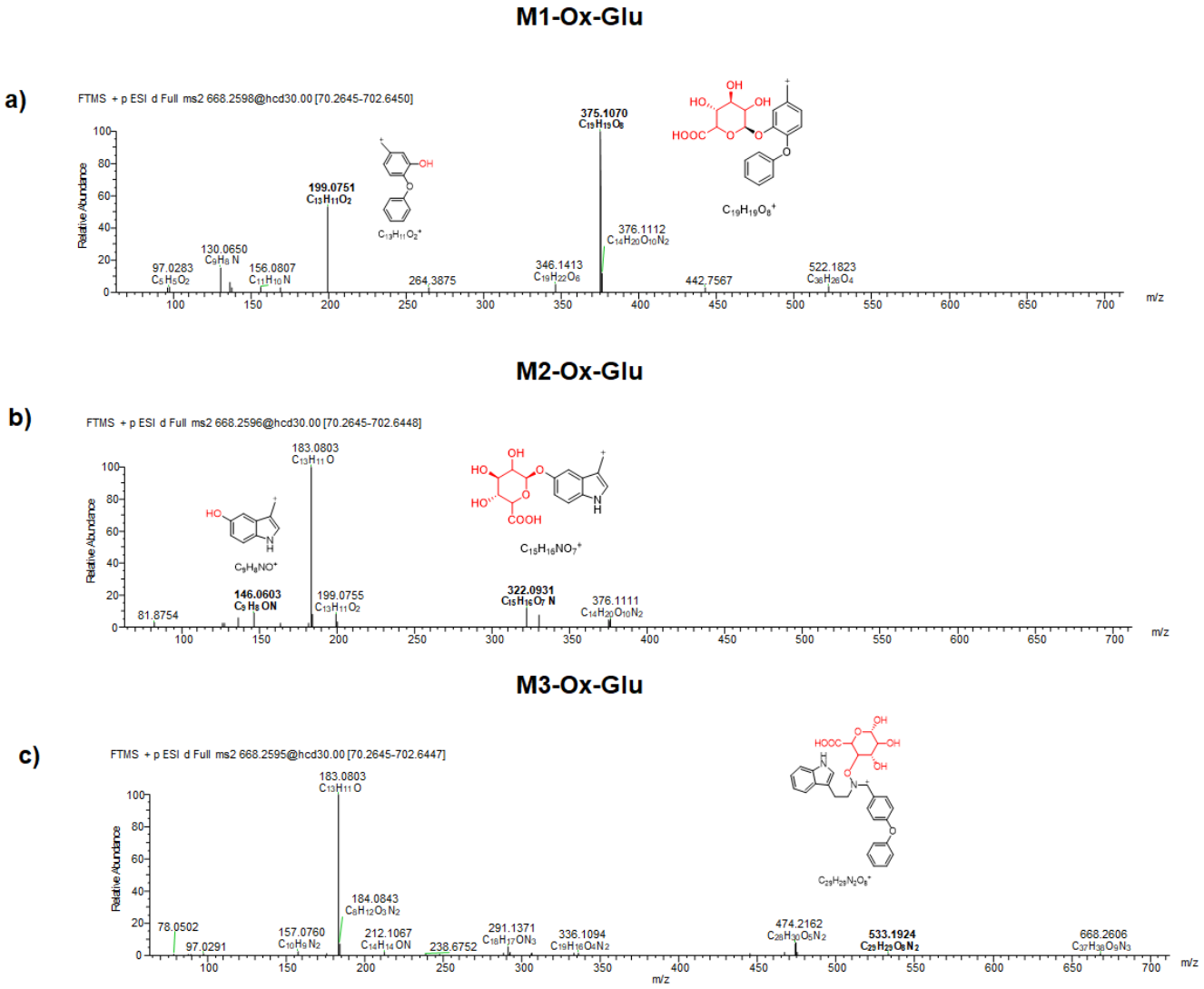

Figure S50: Molecular structures of compound **CPK18** glucuronic metabolites M1-Ox-Glu **(a)**, M2-Ox-Glu **(b)** and M3-Ox-Glu **(c)** as determined by MS/MS analysis